CRACKED ELASTIC ANNULUS BONDED TO RIGID CYLINDER

A THESIS SUBMITTED TO
THE GRADUATE SCHOOL OF NATURAL AND APPLIED SCIENCES
OF
MIDDLE EAST TECHNICAL UNIVERSITY

BY

ENGİN YILMAZ

IN PARTIAL FULFILLMENT OF THE REQUIREMENTS
FOR
THE DEGREE OF MASTER OF SCIENCE
IN
ENGINEERING SCIENCES

DECEMBER 2005

Approval of the Graduate School of Natural and Applied Sciences

Prof. Dr. Canan ÖZGEN
Director

I certify that this thesis satisfies all the requirements as a thesis for the degree of Master of Science.

Prof. Dr. M. Ruşen GEÇİT
Head Of Department

This is to certify that we have read this thesis and that in our opinion it is fully adequate, in scope and quality, as a thesis for the degree of Master of Science.

Prof. Dr. M. Ruşen GEÇİT
Supervisor

Examining Committee Members

Prof. Dr. Cevdet AKGÖZ	(METU, ES)	
Prof. Dr. M. Ruşen GEÇİT	(METU, ES)	
Prof. Dr. Hasan YAZICIGİL	(METU, GEOE)	
Assoc. Prof. Dr. Murat DİCLELİ	(METU, ES)	
Assist. Prof. Dr. Ferhat AKGÜL	(METU, ES)	

I hereby declare that all information in this document has been obtained and presented in accordance with academic rules and ethical conduct. I also declare that, as required by these rules and conduct, I have fully cited and referenced all material and results that are not original to this work.

Name, Last name : Engin YILMAZ

Signature :

ABSTRACT

CRACKED ELASTIC ANNULUS BONDED TO
RIGID CYLINDER

Yılmaz, Engin
Ms., Department of Engineering Sciences
Supervisor: Prof. Dr. M. Ruşen Geçit

December 2005, 71 pages

In this study, a long annulus bonded to a rigid cylinder containing an axisymmetric circumferential crack of width (d-c) at the midplane is considered. The material of the annulus is assumed to be linearly elastic and isotropic. The external surface of the annulus is free of stress. Surfaces of the crack are subject to distributed compressive loads.

The Fourier and Hankel transform techniques are used to solve the governing equations which are reduced to a singular integral equation for crack surface displacement derivative. This integral equation is converted to a system of linear algebraic equations which are solved numerically by using Gauss-Lobatto and Gauss-Jacobi quadrature formulas. Then, the stress intensity factors at the edges of the crack are calculated. Results are presented in graphical form.

Keywords: annulus, rigid cylinder, crack, stress intensity factor.

ÖZ

İÇİNDEN RİJİT SİLİNDİRE YAPIŞAN ÇATLAKLI TÜP

Yılmaz, Engin
Yüksek Lisans, Mühendislik Bilimleri Bölümü
Tez Yöneticisi: Prof. Dr. M. Ruşen Geçit

Aralık 2005, 71 sayfa

Bu çalışmada, içinden rijit silindire yapışan (d-c) genişliğinde halka şeklinde simetrik çatlak içeren iç çapı a, dış çapı b olan bir tüp problemi ele alınmıştır. Tüpün malzemesinin lineer elastik ve izotrop olduğu varsayılmıştır. Tüpün dış yüzeyi serbesttir. Çatlak yüzeyleri yayılı basınç yüklerine maruzdur.

Problemin çözümü sonsuzda düzgün yayılı çekmeye maruz kalmış tüp ve halka şeklinde çatlak içeren tüp problemlerinden elde edilir. Elastisite denklemleri, Fourier ve Hankel dönüşümleri kullanılarak çatlak yüzü yer değiştirme türevi cinsinden yazılan bir tekil integral denkleme dönüştürülür. Gauss-Lobatto ve Gauss-Jacobi integrasyon formülleri kullanılarak bu tekil integral denklem bir lineer cebrik denklem takımına dönüştürülür. Daha sonra çatlak uçlarındaki gerilme şiddeti katsayıları sayısal olarak hesaplanır. Sonuçlar grafikler şeklinde verilmektedir.

Anahtar Kelimeler: sonsuz uzunlukta tüp, çatlak, rijit silindir, gerilme şiddeti katsayısı.

TO MY SISTER

ACKNOWLEDGEMENTS

I have to start by expressing my deepest gratitude to Prof. Dr. M. Ruşen Geçit without whose guidance this work would never have been completed. I am also grateful to Mete and Tarık, my very close friends, who kept me motivated throughout my research. Finally and most importantly, I am grateful to my family, my mother and father in particular, who always supported me in my professional endeavors.

TABLE OF CONTENTS

NOMENCLATURE

d-c	Width of crack
c_1, c_2, c_3, c_4	Arbitrary integration constants
a, b	Inner and outer radii of infinite cylinder
p_0	Nominal compressive load on crack surfaces
r, θ, z	Cylindrical Coordinates
u, w	Displacement components in r- and z-directions
σ, τ	Normal and shear components of stress
κ	3-4ν
μ	Shear modulus of elasticity
ν	Poisson's ratio
α	Hankel transform variable
λ	Fourier transform variable
J_0, J_1	Bessel functions of the first kind of order zero and one
I_0, I_1	Modified Bessel functions of the first kind of order zero and one
K_0, K_1	Modified Bessel functions of the second kind of order zero and one
f(r)	Crack surface displacement derivative
F(α)	Hankel transform of f(r)
G(r)	Hölder-continuous function
K, E	Complete elliptic integrals of the first and the second kinds
N	Kernel of the integral equation
ξ, τ	Normalized variables at z=0
γ	Singularity power
η, ε	Normalized variables at z=0
k_a, k_c, k_d	Mode I stress intensity factors at the tips of the crack
K'(c), k'(d)	Normalized stress intensity factors
$P^{(\alpha, \beta)}$	Jacobi polynomial

CHAPTER I

INTRODUCTION

Despite the early works on understanding of cause of fracture, mathematical relation between fracture stress and flaw size was studied and explained by Griffith whose study, which was a monumental study for the beginning of an understanding of this field, was published in 1920.

In the field of fracture mechanics, axisymmetric problems constitute a major research area. Generally, these types of problems are simplified and formulated in the form of boundary value problems, and solved by either analytical or numerical methods. Obviously, solution for annular domain requires much more complicated calculations compared to circular domain.

This problem will be investigated by studying partial differential equations derived from 3-D elasticity theory and using singular integral equations. Since the geometry and the loading are symmetric about the z-axis, two-dimensional axisymmetric equations and relations will be used.

1.1 Literature review

Sneddon and Welch [1] made an analysis of the distribution of stress in a long circular cylinder of elastic material when it is deformed by the application of pressure to the inner surfaces of a penny-shaped crack situated symmetrically at the center of the cylinder. It is assumed that the cylindrical surface is free from stress. The equations of the classical theory of elasticity are solved in terms of an unknown function which is then shown to be the solution of a Fredholm integral equation of the second kind previously derived by Collins [2]. The solutions of this equation for constant pressure and for various ratios of the radius of the crack to that of the cylinder are derived using a high-speed computer are discussed and quantities of physical interest are calculated. The calculations are repeated for the case of a variable pressure following a parabolic law and they are also reported.

Gupta [3] analyzed a semi-infinite cylinder with fixed short end. Normal loads far away from the fixed end are prescribed. An exact formulation of the problem in terms of a singular integral equation is provided by using an integral transform technique. Stresses along the rigid end and stress intensity factors are computed numerically and are presented graphically.

Geçit [4] analyzed the elastostatic plane problem of an infinite strip containing a transverse crack. It is assumed that one side of the strip is perfectly bonded to rigid support whereas the other side is free of traction. The problem is formulated in terms of a singular integral equation. Internal crack, edge crack, crack terminating at the rigid support, and completely broken strip cases are considered in some detail. The singular integral equation is solved numerically by employing collocation schemes developed by Erdogan, Gupta and Cook [5]. The stress intensity factor, which may be regarded as the most important fracture parameter, and the crack surface displacement are calculated for various crack geometries and given in graphical form.

Agarwall [6] states that axisymmetric end-problem for a semi-infinite elastic circular cylinder is reduced to a system of singular integral equations, using transform methods. The kernels of the integral equations are found to contain Cauchy as well as generalized Cauchy-type singularities. The dominant part of the equations is separated and analyzed to determine the index of the singularity for differing boundary conditions at the end. An approximate method is used to obtain a system of simultaneous algebraic equations from the system of singular integral equations. As an application, axisymmetric solution for joined dissimilar elastic semi-infinite cylinders under uniform tension is solved and various physical quantities of interest, such as normal and shear stresses at the interface are obtained.

Delale and Erdogan [7] formulated the plane elasticity problem for a hollow cylinder or a disk containing a radial crack is given. The crack may be an external edge crack, internal edge crack, or and embedded crack. It is assumed that on the crack surfaces the shear traction is zero and the normal traction is an arbitrary function of r. For various crack geometries and radius ratios, the numerical results are obtained for a uniform crack surface pressure, for a uniform pressure acting on the inside wall of the cylinder, and for a rotating disk.

Nied and Erdogan [8] analyzed the elasticity problem for a long hollow circular cylinder containing an axisymmetric circumferential crack subject to general nonaxisymmetric external loads. The problem is formulated in terms of a system of singular integral equations with the Fourier coefficients for the derivative of the crack surface displacement as density functions. The stress intensity factors and the crack opening displacement are calculated for a cylinder under uniform tension, bending by end couples, end self-equilibrating residual stresses.

Altundağ Artem and Geçit [9] analyzed the fracture of an axisymmetric hollow cylindrical bar containing rigid inclusions. The cylinder is under the action of uniformly distributed axial tension applied at infinity. The bar contains a ring-shaped crack at the symmetry plane whose surface are free of tractions and two ring-shaped rigid inclusions with negligible thickness symmetrically located on both sides of the crack. It is assumed that the material of the cylinder is linearly elastic and isotropic.

The mixed boundary conditions of the problem lead the analysis to a system of three singular integral equations for crack surface displacement derivative and normal and shearing stress jumps on rigid inclusions. These integral equations are solved numerically and stress intensity factors are calculated.

Toygar and Geçit [10] analyzed the problem of an axisymmetric infinite cylinder with a ring shaped crack at $z = 0$ and two ring-shaped rigid inclusions with negligible thickness at $z = \pm L$. The cylinder is under the action of uniformly distributed axial tension applied at infinity and its lateral surface is free of traction. It is assumed that the material of the cylinder is linearly elastic and isotropic. Crack surfaces are free and the constant displacements are continuous along the rigid inclusions while the stresses have jumps. Formulation of the mixed boundary value problem under consideration is reduced to three singular integral equations in terms of the derivative of the crack surface displacement and the stress jumps on the rigid inclusions. These equations, together with the single-valuedness condition for the displacements around the crack and the equilibrium equations along the inclusions are converted to a system of linear algebraic equations, which is solved numerically. Stress intensity factors are calculated and presented in graphical form.

Birinci [11] analyzed the elastostatic axisymmetric problem for a long-thick walled cylinder containing an axisymmetric circumferential internal or edge crack with cladding. The cladding is assumed to be bonded to inner wall of the hollow cylinder. Using the standard transform technique, the problem is formulated in terms of an integral equation of the first kind which has a generalized Cauchy kernel as the dominant part. The integral equation is solved numerically by using appropriate quadrature formulas. The related stress intensity factors are calculated for the hollow cylinder with the cladding under axial load.

1.2 A Short Introduction and Method of Solution of the Problem

The aim of this study is to investigate the stress intensity factors for an infinite annulus containing circumferential internal or edge crack bonded to rigid cylinder and with traction free external surface. The material of the annulus is assumed to be linearly elastic and isotropic. The solution of this problem can be obtained by superposition of solutions for; (i) an infinite annulus bonded to rigid cylinder containing an axisymmetric circumferential crack of width (d-c) at the midplane, (ii) an infinite annulus bonded to rigid cylinder subjected to arbitrary axisymmetric loads.

Displacement and stress components for this perturbation problem are obtained by using Fourier and Hankel transform techniques in the solution of field equations.

Formulation will be reduced to a singular integral equation in terms of the crack surface displacements derivative by applying the boundary conditions. This singular integral equation will be converted to a system of linear algebraic equations to be solved numerically by using Gauss-Lobatto and Gauss-Jacobi integration formulas.

CHAPTER II

FORMULATION OF THE PROBLEM

2.1 The Cracked Infinite Elastic Annulus Bonded to Rigid Cylinder Problem

A long cracked elastic annulus bonded to rigid cylinder subject to distributed compressive load on the crack surfaces (See Figure 1) is considered. The material of the annulus is assumed to be linearly elastic and isotropic. The external surface of the annulus is free of stress. The annulus of inner and outer radii a and b contains a ring-shaped plane crack of inner and outer radii c and d at z=0 plane. The surfaces of the crack is under the action of distributed compressive loads p(r).

For linearly elastic, isotropic and axisymmetric elasticity problems, the field equations can be listed in the form:

Stress-displacement relations:

$$\sigma_r = \frac{\mu}{\kappa-1}\left[(\kappa+1)\frac{\partial u}{\partial r} + (3-\kappa)\left(\frac{u}{r} + \frac{\partial w}{\partial z}\right)\right],$$

$$\sigma_\theta = \frac{\mu}{\kappa-1}\left[(\kappa+1)\frac{u}{r} + (3-\kappa)\left(\frac{\partial u}{\partial r} + \frac{\partial w}{\partial z}\right)\right],$$

$$\sigma_z = \frac{\mu}{\kappa-1}\left[(\kappa+1)\frac{\partial w}{\partial z} + (3-\kappa)\left(\frac{\partial u}{\partial r} + \frac{u}{r}\right)\right],$$

$$\tau_{rz} = \mu\left(\frac{\partial u}{\partial z} + \frac{\partial w}{\partial r}\right), \qquad (2.1\text{ a-d})$$

where u, w are displacements in r and z directions in cylindrical coordinate system, μ is the shear modulus, κ = 3 – 4ν, ν being the Poisson's ratio, σ and τ denote the normal and shearing stresses.

Navier equations:

$$(\kappa+1)\left(\frac{\partial^2 u}{\partial r^2}+\frac{1}{r}\frac{\partial u}{\partial r}-\frac{u}{r^2}\right)+(\kappa-1)\frac{\partial^2 u}{\partial z^2}+2\frac{\partial^2 w}{\partial r\partial z}=0\,,$$

$$2\left(\frac{\partial^2 u}{\partial r\partial z}+\frac{1}{r}\frac{\partial u}{\partial z}\right)+(\kappa-1)\left(\frac{\partial^2 w}{\partial r^2}+\frac{1}{r}\frac{\partial w}{\partial r}\right)+(\kappa+1)\frac{\partial^2 w}{\partial z^2}=0\,. \qquad (2.2\text{ a, b})$$

These equations must be solved subject to the following boundary conditions:

$$\sigma_z(r, \pm\infty)=0\,,$$
$$w(r,\ 0)=0\,, \qquad (a<r<c, \quad d<r<b)\,,$$
$$\sigma_z(r, 0)=-p(r)\,, \qquad (c<r<d)\,,$$
$$w(a,\ z)=0\,, \qquad (-\infty<z<\infty)\,,$$
$$\tau_{rz}(b, z)=0 \qquad (-\infty<z<\infty)\,,$$
$$u(a,\ z)=0 \qquad (-\infty<z<\infty)\,,$$
$$\sigma_r(b, z)=0 \qquad (-\infty<z<\infty)\,. \qquad (2.3\text{ a-g})$$

General expressions for the displacement and stress components for this perturbation problem may be obtained by adding the general expressions for (i) an infinite annulus bonded to rigid cylinder containing an axisymmetric circumferential crack of width (d-c) at the midplane, (ii) an infinite annulus bonded to rigid cylinder subjected to arbitrary axisymmetric loads. The informal superposition scheme is given in Figure 2. This is necessary in order to obtain general expressions containing sufficient number of unknown quantities so that all of the boundary conditions in Eq. (2.3) can be satisfied.

2.1.1 Cracked Infinite Elastic Annulus Bonded to Rigid Cylinder

Considering an axisymmetric half space ($z \geq 0$) and taking H_1 Hankel transform [9] of Eq. (2.2a) and H_0 Hankel transform of Eq.(2.2b) in r-direction, and combining the resulting equations, one obtains

$$\frac{d^4U}{dz^4} - 2\alpha^2 \frac{d^2U}{dz^2} + \alpha^4 U = 0, \qquad (2.4)$$

where α is the Hankel transform variable, U(α, z) is H_1 Hankel transform of u(r, z):

$$U(\alpha, z) = \int_0^\infty u(r, z) r J_1(\alpha r) dr, \qquad (2.5)$$

where J_1 denotes the Bessel function of the first kind of order one.
The general solution of Eq. (2.4) is:

$$U(\alpha, z) = (c_1 + c_2 z)e^{-\alpha z} + (c_3 + c_4 z)\, e^{\alpha z}, \qquad (2.6)$$

where c_1, c_2, c_3 and c_4 are arbitrary constants. In order to have finite displacements at z=∞, c_3 and c_4 must be zero. Therefore, for the upper half space,

$$U_1(\alpha, z) = (c_1 + c_2 z)\, e^{-\alpha z}, \qquad (2.7a)$$

and similarly

$$W_1(\alpha, z) = \left[(c_1 + c_2 z) + \frac{\kappa}{\alpha} c_2 \right] e^{-\alpha z}, \qquad (2.7b)$$

where the subscript 1 indicates the upper half-space.

Taking the inverse transform of Eqs.(2.7), displacement components are found to be

$$u_1(r,z)=\int_0^{\infty}(c_1+c_2 z)\,e^{-\alpha z}\alpha J_1(\alpha r)d\alpha\,,$$

$$w_1(r,z)=\int_0^{\infty}\left[(c_1+c_2 z)+\frac{\kappa}{\alpha}c_2\right]e^{-\alpha z}\alpha J_0(\alpha r)d\alpha\,, \qquad \text{(2.8a, b)}$$

where J_0 and J_1 are the Bessel functions of the first kind of order zero and one, respectively. Substituting Eqs. (2.8) in Eqs. (2.1), one obtains the following expressions for the stress components:

$$\sigma_{r1}(r,z)=\mu\int_0^{\infty}(-2)\,(c_1+c_2 z)\,e^{-\alpha z}\frac{\alpha}{r}J_1(\alpha r)d\alpha$$

$$+\mu\int_0^{\infty}\left[2\alpha(c_1+c_2 z)-(3-\kappa)c_2\right]e^{-\alpha z}\alpha J_0(\alpha r)d\alpha,$$

$$\sigma_{z1}(r,z)=\mu\int_0^{\infty}\left[-2\alpha(c_1+c_2 z)-(\kappa+1)c_2\right]e^{-\alpha z}\alpha J_0(\alpha r)d\alpha\,,$$

$$\tau_{rz1}(r,z)=\mu\int_0^{\infty}\left[-2\alpha(c_1+c_2 z)-(\kappa-1)c_2\right]e^{-\alpha z}\alpha J_1(\alpha r)d\alpha\,. \qquad \text{(2.9a, c)}$$

By a similar procedure the expressions for the displacements and stresses for the lower half space are obtained in the form:

$$u_2(r,z)=\int_0^{\infty}(c_3+c_4 z)\,e^{\alpha z}\alpha J_1(\alpha r)d\alpha\,,$$

$$w_2(r,z)=\int_0^{\infty}\left[-(c_3+c_4 z)+\frac{\kappa}{\alpha}c_4\right]e^{\alpha z}\alpha J_0(\alpha r)d\alpha\,. \qquad \text{(2.10a, b)}$$

$$\sigma_{r2}(r,z)=\mu\int_0^{\infty}-2(c_3+c_4z)\,e^{\alpha z}\,\frac{\alpha}{r}J_1(\alpha r)d\alpha$$
$$+\mu\int_0^{\infty}\left[2\alpha(c_3+c_4z)+(3-\kappa)c_4\right]e^{\alpha z}\alpha J_0(\alpha r)d\alpha,$$

$$\sigma_{z2}(r,z)=\mu\int_0^{\infty}\left[-2\alpha(c_3+c_4z)+(\kappa+1)c_4\right]e^{\alpha z}\alpha J_0(\alpha r)d\alpha\,,$$

$$\tau_{rz2}(r,z)=\mu\int_0^{\infty}\left[2\alpha(c_3+c_4z)-(\kappa-1)c_4\right]e^{\alpha z}\alpha J_1(\alpha r)d\alpha\,, \qquad (2.11\text{a, c})$$

where the subscript 2 denotes the lower half space. These expressions may be matched on the z=0 plane by the following continuity and symmetry conditions:

$$\sigma_{z1}(r,0)=\sigma_{z2}(r,0)\,, \qquad (0\le r<\infty),$$
$$\tau_{rz1}(r,0)=\tau_{rz2}(r,0)\,, \qquad (0\le r<\infty),$$
$$u_1(r,0)=u_2(r,0)\,, \qquad (0\le r<\infty),$$
$$w_1(r,0)=w_2(r,0)\,, \qquad (0\le r<c,\quad d<r<\infty),$$
$$\sigma_z(r,0)=-p(r)\,. \qquad (c<r<d). \qquad (2.12\text{a-e})$$

In order to have conditions of the same type, conditions (2.12c,d) may be replaced by

$$\frac{\partial}{\partial r}\left[u_1(r,0)-u_2(r,0)\right]=0\,, \qquad (0\le r<\infty),$$
$$\frac{\partial}{\partial r}\left[w_1(r,0)-w_2(r,0)\right]=2f(r)\,, \qquad (0\le r<\infty). \qquad (2.13\text{a, b})$$

where f(r) is an unknown function such that f(r)=0 when $(0\le r<a,\quad d<r<\infty)$.

Now substituting Eqs.(2.8) through (2.10) in Eqs.(2.12a-b) and (2.13) one obtains the unknown constants

$$c_1 = c_3 = \frac{(\kappa - 1)}{(\kappa + 1)} \frac{F(\alpha)}{\alpha},$$

$$c_2 = -c_4 = -\frac{2F(\alpha)}{(\kappa + 1)}, \tag{2.14a, b}$$

where

$$F(\alpha) = \int_0^\infty f(r) r J_1(\alpha r) dr. \tag{2.15}$$

Note that the cracked elastic annulus is symmetric about z-axis and also z=0 plane. Therefore, it is sufficient to consider the axisymmetric problem in the upper half z≥0 only. The displacements and the stresses for the problem will then be

$$u(r,z) = \frac{1}{\kappa + 1} \int_0^\infty (\kappa - 1 - 2\alpha z) F(\alpha)\, e^{-\alpha z} J_1(\alpha r) d\alpha,$$

$$w(r,z) = \frac{1}{\kappa + 1} \int_0^\infty (-\kappa - 1 + 2\alpha z) F(\alpha)\, e^{-\alpha z} J_0(\alpha r) d\alpha. \tag{2.16a, b}$$

$$\sigma_r(r,z) = \frac{2\mu}{\kappa + 1} \left\{ \begin{array}{l} \int_0^\infty (-\kappa + 1 + 2\alpha z) F(\alpha)\, e^{-\alpha z} \frac{1}{r} J_1(\alpha r) d\alpha \\ + \int_0^\infty 2(1 - \alpha z) F(\alpha)\, e^{-\alpha z} \alpha J_0(\alpha r) d\alpha \end{array} \right\},$$

$$\sigma_z(r,z) = \frac{4\mu}{\kappa + 1} \int_0^\infty (1 + \alpha z) F(\alpha)\, e^{-\alpha z} \alpha J_0(\alpha r) d\alpha,$$

$$\tau_{rz}(r,z) = \frac{4\mu}{\kappa + 1} \int_0^\infty \alpha^2 z F(\alpha)\, e^{-\alpha z} J_1(\alpha r) d\alpha. \tag{2.17a-c}$$

2.1.2 Infinite Elastic Annulus Bonded to Rigid Cylinder without Crack

Consider an infinite medium without crack loaded axisymmetrically. Medium is symmetric about both z-axis and z=0 plane. Now taking the Fourier cosine transform of Eq.(2.2a) and sine transform of Eq.(2.2b) in z-direction and combining again the resulting equations, one obtains

$$\left[x^4\frac{d^4}{dx^4}+2x^3\frac{d^3}{dx^3}-(2x^4+3x^2)\frac{d^2}{dx^2}-(2x^3+3x)\frac{d}{dx}+(x^4+2x^2-3)\right]U_c=0, \tag{2.18}$$

where U_c is the Fourier cosine transform of the displacement component u(r, z) in which x = λr, λ being the Fourier transform variable.

Solution of Eq. (2.18) is [13, 14]:

$$U_c=c_1I_1(\lambda r)+c_2K_1(\lambda r)+c_3\lambda rI_0(\lambda r)+c_4\lambda rK_0(\lambda r), \tag{2.19}$$

where I_0, K_0, I_1 and K_1 are the modified Bessel functions of the first and the second kinds of order zero and one, respectively and c_1, c_2, c_3 and c_4 are arbitrary constants.

Similarly, from Fourier transform of Eqs.(2.2)

$$\begin{aligned}W_s=&-c_1I_0(\lambda r)+c_2K_0(\lambda r)-c_3\left[(\kappa+1)I_0(\lambda r)+\lambda rI_1(\lambda r)\right]\\&-c_4\left[(\kappa+1)K_0(\lambda r)-\lambda rK_1(\lambda r)\right]\end{aligned}, \tag{2.20}$$

where the subscript s implies the sine transform.

Taking the inverse transforms of Eqs.(2.19) and (2.20), expressions for the displacement components are found to be

$$u(r,z)=\frac{2}{\pi}\int_0^\infty\left\{c_1 I_1(\lambda r)+c_2 K_1(\lambda r)+c_3\lambda r I_0(\lambda r)+c_4\lambda r K_0(\lambda r)\right\}\cos(\lambda z)d\lambda\,,$$

$$w(r,z)=\frac{2}{\pi}\int_0^\infty\left\{\begin{matrix}-c_1 I_0(\lambda r)+c_2 K_0(\lambda r)-c_3\left[(\kappa+1)I_0(\lambda r)+\lambda r I_1(\lambda r)\right]\\ -c_4\left[(\kappa+1)K_0(\lambda r)-\lambda r K_1(\lambda r)\right]\end{matrix}\right\}\sin(\lambda z)d\lambda\,.$$

(2.21a, b)

Substituting Eqs. (2.21) in Eqs. (2.1) one obtains the following expressions for the stress components:

$$\sigma_r(r,z)=\frac{2\mu}{\pi}\int_0^\infty\left\{\begin{matrix}c_1\left[-\frac{2}{r}I_1(\lambda r)+2I_0(\lambda r)\lambda\right]+c_2\left[-\frac{2}{r}K_1(\lambda r)-2K_0(\lambda r)\lambda\right]\\ +c_3\left[\lambda I_0(\lambda r)(\kappa-1)+2I_1(\lambda r)\lambda^2 r\right]\\ +c_4\left[\lambda K_0(\lambda r)(\kappa-1)-2K_1(\lambda r)\lambda^2 r\right]\end{matrix}\right\}\cos(\lambda z)d\lambda\,,$$

$$\sigma_z(r,z)=\frac{2\mu}{\pi}\int_0^\infty\left\{\begin{matrix}-2c_1 I_0(\lambda r)\lambda+2c_2 K_0(\lambda r)\lambda\\ -c_3\left[I_0(\lambda r)(\kappa+5)\lambda+2I_1(\lambda r)\lambda^2 r\right]\\ -c_4\left[K_0(\lambda r)(\kappa+5)\lambda-2K_1(\lambda r)\lambda^2 r\right]\end{matrix}\right\}\cos(\lambda z)d\lambda\,,$$

$$\tau_{rz}(r,z)=\frac{2\mu}{\pi}\int_0^\infty\left\{\begin{matrix}-2c_1 I_1(\lambda r)\lambda-2c_2 K_1(\lambda r)\lambda\\ -c_3\left[I_1(\lambda r)(\kappa+1)\lambda+2I_0(\lambda r)\lambda^2 r\right]\\ +c_4\left[K_1(\lambda r)(\kappa+1)\lambda-2K_0(\lambda r)\lambda^2 r\right]\end{matrix}\right\}\sin(\lambda z)d\lambda\,\cdot$$

(2.22a-c)

2.1.3 General Solution

General expressions for displacement and stress components obtained in previous sections will be added together for the solution of the perturbation problem:

$$u(r,z) = u_{crack} + u_{fourier} ,$$

$$w(r,z) = w_{crack} + w_{fourier} . \qquad (2.23a, b)$$

$$\sigma_z(r,z) = \sigma_{z\,crack} + \sigma_{z\,fourier} ,$$

$$\tau_{rz}(r,z) = \tau_{rz\,crack} + \tau_{rz\,fourier} ,$$

$$\sigma_r(r,z) = \sigma_{r\,crack} + \sigma_{r\,fourier} . \qquad (2.24a-c)$$

Four unknown constants c_1-c_4 appearing in Fourier transform solution can be expressed in terms of the unknown function F(α) using the following conditions at inner and outer lateral surfaces of the annulus:

$$w(a,z) = 0 ,$$

$$\tau_{rz}(b,z) = 0 ,$$

$$u(a,z) = 0 ,$$

$$\sigma_r(b,z) = 0 . \qquad (2.25a-d)$$

Therefore, substituting Eqs. (2.17), (2.22) in Eqs. (2.25) and using the integral formulas given by (A.1) in Appendix A, the following algebraic equations for c_1-c_4 are obtained:

$$\frac{1}{\kappa+1}\int_0^\infty F(\alpha)J_0(A\alpha)\left[\frac{4\alpha^2\lambda}{\left(\lambda^2+\alpha^2\right)^2}+(\kappa+1)\frac{\lambda}{\lambda^2+\alpha^2}\right]d\alpha=-c_1I_0(A\lambda)+c_2K_0(A\lambda)$$
$$-c_3\left[(\kappa+1)I_0(A\lambda)+A\lambda I_1(A\lambda)\right]-c_4\left[(\kappa+1)K_0(A\lambda)-A\lambda K_1(A\lambda)\right]\quad,$$
$$\frac{4}{\kappa+1}\int_0^\infty F(\alpha)J_1(B\alpha)\frac{2\alpha^3}{\left(\lambda^2+\alpha^2\right)^2}d\alpha=2c_1I_1(B\lambda)+2c_2K_1(B\lambda)$$
$$+c_3\left[I_1(B\lambda)(\kappa+1)+2I_0(B\lambda)\lambda B\right]-c_4\left[K_1(B\lambda)(\kappa+1)-2K_0(B\lambda)\lambda B\right]\quad,$$
$$\frac{1}{\kappa+1}\int_0^\infty F(\alpha)J_1(A\alpha)\alpha\left[\frac{2\left(\alpha^2-\lambda^2\right)}{\left(\lambda^2+\alpha^2\right)^2}-(\kappa-1)\frac{1}{\lambda^2+\alpha^2}\right]d\alpha=$$
$$c_1I_1(A\lambda)+c_2K_1(A\lambda)+c_3\lambda AI_0(A\lambda)+c_4\lambda AK_0(A\lambda)\quad,$$
$$\frac{1}{\kappa+1}\int_0^\infty F(\alpha)\left\{J_1(B\alpha)\alpha\left[\frac{2\left(\lambda^2-\alpha^2\right)}{\left(\lambda^2+\alpha^2\right)^2}+\frac{\kappa-1}{\lambda^2+\alpha^2}\right]+2J_0(B\alpha)B\alpha^2\left[\frac{\alpha^2-\lambda^2}{\left(\lambda^2+\alpha^2\right)^2}-\frac{1}{\lambda^2+\alpha^2}\right]\right\}d\alpha=$$
$$c_1\left[-I_1(B\lambda)+BI_0(B\lambda)\lambda\right]+c_2\left[-K_1(B\lambda)-BK_0(B\lambda)\lambda\right]$$
$$+c_3\left[\lambda\frac{B}{2}I_0(B\lambda)(\kappa-1)+I_1(B\lambda)\lambda^2B^2\right]+c_4\left[\lambda\frac{B}{2}K_0(B\lambda)(\kappa-1)-K_1(B\lambda)\lambda^2B^2\right]\quad.$$

(2.26a-d)

These equations are solved and following expressions are obtained:

$$c_1=\left[c_{11}F_1+c_{12}F_2+c_{13}F_3+c_{14}F_4\right]/D,$$
$$c_2=\left[c_{21}F_1+c_{22}F_2+c_{23}F_3+c_{24}F_4\right]/D,$$
$$c_3=\left[c_{31}F_1+c_{32}F_2+c_{33}F_3+c_{34}F_4\right]/D,$$
$$c_4=\left[c_{41}F_1+c_{42}F_2+c_{43}F_3+c_{44}F_4\right]/D.\qquad(2.27a\text{-}d)$$

where F_1-F_4 are given by (B.1), c_{11}-c_{44} and D are given by (B.3) in Appendix B.

The boundary conditions on the inner and outer lateral surfaces of the elastic annulus have already been used in finding expressions for c_1-c_4. The remaining boundary condition Eq. (2.3c) is used to determine the unknown function f(r).

CHAPTER III

INTEGRAL EQUATIONS

3.1 Derivation of Integral Equations

The expression for σ_{z}, u and w in terms of unknown function $f(t)$ when substituted in Eqs. (2.3c) give the following singular integral equation with kernel having Cauchy-type singularity [12]:

$$\frac{2\mu}{\pi(\kappa+1)}\int_{c}^{d} f(t)\left[\frac{2}{t-r}+2M(r,t)+tN(r,t)\right]dt=-p(r), \qquad c<r<d \tag{3.1}$$

where

$$M(r,t)=\frac{M^{*}(r,t)-1}{t-r} \quad , \tag{3.2}$$

and

$$M^{*}(r,t)=\begin{cases}\dfrac{2(t-r)}{r}K(\dfrac{t}{r})+\dfrac{2r}{(t+r)}E(\dfrac{t}{r}) & (r>t)\\ \dfrac{2t}{t+r}E(\dfrac{t}{r}) & (r<t)\end{cases}, \tag{3.3}$$

in which K and E are the complete elliptic integrals of the firs and the second kinds, respectively.

The kernel N is defined as follows:

$$N(r,t)=\int_0^{\infty} L(r,t,\lambda)\,d\lambda \tag{3.4}$$

where $L(r,t,\lambda)$ may be obtained in the form:

$$L(r,t,\lambda)=(\kappa+1)\begin{Bmatrix}-2c_1 I_0(\lambda r)\lambda+2c_2K_0(\lambda r)\lambda-c_3\left[I_0(\lambda r)(\kappa+5)\lambda+2I_1(\lambda r)\lambda^2 r\right]\\ -c_4\left[K_0(\lambda r)(\kappa+5)\lambda-2K_1(\lambda r)\lambda^2 r\right]\end{Bmatrix} \tag{3.5}$$

where c_1, c_2, c_3 and c_4 are given in Eqs. (2.27 a-d).

The integral equation, Eq. (3.1), must be solved by using single valuedness condition for crack:

$$\int_c^d f(t)\,dt=0. \tag{3.6}$$

The integral equation have i) a simple Cauchy type singularity at t=r, ii) the kernel M have logarithmic singularity, iii) the Fredholm kernel N has singular terms when t=a,b and r=a, b due to the behavior of integrand of the integral giving N as $\lambda\rightarrow\infty$. Therefore, N(r, t) can be written in the following form

$$N(r,t)=\int_0^{\infty} L(r,t,\lambda)\,d\lambda\,. \tag{3.7}$$

Then, the singular part of the kernel may be separated as

$$N_s(r,t)=\int_0^{\infty} L_{\infty}(r,t,\lambda)\,d\lambda\,, \tag{3.8}$$

where

$$L_{\infty}(r,t,\lambda)=\lim_{\lambda\to\infty}L(r,t,\lambda)\,. \tag{3.9}$$

Integrand of integral given by Eq. (3.7) contains modified Bessel functions. By using asymptotic expansions for modified Bessel functions, the expression for $L_{\infty}(r, t, \lambda)$ may be obtained in the form

$$L_{\infty}(r,t,\lambda)=\frac{1}{\sqrt{rt}}\left\{\begin{aligned}&e^{-\lambda(2b-r-t)}\left[-4+(8b-2r-6t)\lambda-4(b-r)(b-t)\lambda^2\right]\\&+\frac{1}{\kappa}e^{\lambda(2a-r-t)}\left[-(3+\kappa^2)-(8a-2r-6t)\lambda-4(a-r)(a-t)\lambda^2\right]\end{aligned}\right\}\,. \tag{3.10}$$

The singular part of the kernel N_s can be obtained by integrating L_{∞} with the formulas given in Appendix A by (A.1):

$$N_s(r,t)=\frac{1}{\sqrt{rt}}\left\{\begin{aligned}&\left[-2+12(b-r)\frac{d}{dr}-4(b-r)^2\frac{d^2}{dr^2}\right]\frac{1}{-2b+r+t}\\&+\frac{1}{\kappa}\left[(3-\kappa^2)-12(a-r)\frac{d}{dr}+4(a-r)^2\frac{d^2}{dr^2}\right]\frac{1}{-2a+r+t}\end{aligned}\right\} \tag{3.11}$$

and the bounded part of the kernel will be

$$N_b(r,t)=\int_0^{\infty}\left[L(r,t,\lambda)-L_{\infty}(r,t,\lambda)\right]d\lambda \tag{3.12}$$

Then, the kernel N(r, t) may be written as

$$N(r,t)=N_s(r,t)+N_b(r,t)\,. \tag{3.13}$$

Therefore, Eq. (3.1) may be written in the form

$$\frac{2\mu}{\pi(\kappa+1)}\int_c^d f(t)\left[\frac{2}{t-r}+tN_s(r,t)\right]dt=B(r) \qquad c<r<d \qquad (3.14)$$

where B(r) contains all bounded terms in Eq. (3.1).

Singular behavior of the unknown function f(t) may be determined by writing

$$f(t)=G(t)\left[(t-c)(d-t)\right]^{-\gamma} \qquad 0<\mathrm{Re}(\gamma)<1 \qquad (3.15)$$

where G(t) is Hölder-continuous function in the interval [c, d]. γ is unknown constant.

Evaluating the integrals containing the term 1/(t-r) and using the technique given in [15] near the end points r=c, d

$$\frac{1}{\pi}\int_c^d \frac{f(t)}{t-r}=\frac{F(c)\cot(\pi\gamma)}{\left[(d-c)(r-c)\right]^{\gamma}}-\frac{F(d)\cot(\pi\gamma)}{\left[(d-c)(d-r)\right]^{\gamma}}+F^*(r) \qquad (3.16)$$

is obtained where $F^*(r)$ is bounded everywhere except at the end points c, d. Substituting Eq. (3.16) in Eq. (3.14), following complex function technique outlined in Muskhelishvili [15] and using the procedure described in [16] one may obtain the following characteristic equation for γ

$$\cot(\pi\gamma)=0 \qquad (3.17)$$

Therefore γ=1/2 satisfies the equation above at the tips of the crack (r → c,d).

3.2 Solution of Integral Equation

Defining non-dimensional variables τ, ξ for crack by

$$t=\frac{d-c}{2}\tau+\frac{d+c}{2}, \qquad (c<t<d,\quad -1<\tau<1)$$

$$r=\frac{d-c}{2}\xi+\frac{d+c}{2}. \qquad (c<r<d,\quad -1<\xi<1) \qquad (3.18\text{ a, b})$$

singular integral equation, Eq. (3.1), takes the following form

$$\frac{1}{\pi}\int_{-1}^{+1}\bar{f}(\tau)\left[\frac{2}{\tau-\xi}+\hat{M}(\xi,\tau)+\hat{N}(\xi,\tau)\right]d\tau=-\frac{\bar{p}(\xi)}{2\mu}(\kappa+1) \qquad (-1<\xi<1) \qquad (3.19)$$

where

$$\bar{p}(\xi)=p(\frac{d-c}{2}\xi+\frac{d+c}{2}),$$

$$\bar{f}(\tau)=f(\frac{d-c}{2}\tau+\frac{d+c}{2}) \qquad (3.20\text{a, b})$$

Substituting singular behavior of the dimensionless unknown function

$$\bar{f}(\tau)=\bar{F}(\tau)\left(1-\tau^2\right)^{-1/2}, \qquad (-1<\tau<1) \qquad (3.21)$$

in Eq. (3.19), one may obtain the following integral equation

$$\frac{1}{\pi}\int_{-1}^{1}\frac{\bar{F}(\tau)}{\sqrt{(1-\tau^2)}}\left[\frac{2}{\tau-\xi}+\hat{M}(\xi,\tau)+\hat{N}(\xi,\tau)\right]d\tau=-\frac{\bar{p}(\xi)}{2\mu}(\kappa+1) \qquad (-1<\xi<1) \qquad (3.22)$$

where $\overline{F}(\tau)$, is Hölder-continuous function. This equation, Eq. (3.22), can be reduced to the following system of algebraic equation by using the Gauss-Lobatto integration formula given in [14]:

$$\sum_{i=1}^{n} C_i \overline{F}(\tau_i) \left[\frac{2}{\tau_i - \xi_j} + \hat{M}(\xi_j, \tau_i) + \hat{N}(\xi_j, \tau_i) \right] = -\frac{\overline{p}(\xi)}{2\mu}(\kappa + 1) \quad (j = 1,2,......n-1) \quad (3.23)$$

where

$$\tau_i = \cos\left(\frac{i-1}{n-1} \pi \right) \qquad (i = 1,2,..........n)$$

$$\xi_j = \cos\left(\frac{2j-1}{2(n-1)} \pi \right) \qquad (j = 1,2,..........n-1) \qquad (3.24a, b)$$

are the roots and

$$C_1 = C_2 = \frac{1}{2(n-1)},$$

$$C_i = \frac{1}{n-1} \qquad (i = 2,3,..........n-1) \qquad (3.25a, b)$$

are the weighting constants of related Lobatto polynomials. The equation, Eq. (3.22) contains (n-1) equation for n unknowns, $\overline{F}(\tau_i)$ $(i = 1,2,..........n)$. To complete the system of n equation for n unknowns, the single valuedness and equilibrium conditions, Eq. (3.6), must be taken into consideration. Therefore, Eq. (3.6) become

$$\sum_{i=1}^{n} C_i \overline{F}(\tau_i) = 0 \qquad (-1 < \tau < 1) \qquad (3.26)$$

Infinite integrals with Fredholm kernels, $\hat{N}$ appearing in Eq. (3.23) can be calculated numerically by using Laguerre [14] and Filon [14] integration methods for each τ_i

value. After determining unknowns $\bar{F}(\tau_i)$ $(i = 1,2,..........n)$ at discrete collocation points the field quantities can be computed numerically. Behavior of these unknown functions at the tips of the crack, τ=±1 is characterized by the so-called ‘‘stress intensity factor’’ which is particularly important from the viewpoint of fracture mechanics.

3.3 Stress Intensity Factors

3.3.1 Stress Intensity Factors for the Case of Internal Crack $(a < c < d < b)$

Mode I stress intensity factor at the tips of the crack may be defined as [15]

$$k_c = \lim_{r \to c} \sqrt{2(c-r)}\,\sigma_z(r,0)$$
$$k_d = \lim_{r \to d} \sqrt{2(r-d)}\,\sigma_z(r,0) \qquad (3.27a, b)$$

where $\sigma_z(r,0)$ is given by Eq. (3.1):

$$\sigma_z(r,0) = \frac{4\mu}{\pi(\kappa+1)} \int_c^d \frac{f(t)}{t-r}\, dt + \sigma_{zb}(r,0) \qquad (3.28)$$

where σ_{zb} is the bounded part of the cleavage stress.

$$\sigma_{zb} = \frac{2\mu}{\pi(\kappa+1)} \int_c^d f(t)\left[2M(r,t) + tN(r,t)\right] dt \qquad (3.29)$$

Considering

$$f(t)=\frac{f^*(t)}{\sqrt{(t-c)(d-t)}}=\begin{cases}\dfrac{f^*(t)/\sqrt{(d-t)}}{\sqrt{(t-c)}} & near\ c \\ \dfrac{f^*(t)/\sqrt{(t-c)}}{\sqrt{(t-d)}} & near\ d\end{cases} \tag{3.30}$$

The integral of the sectionally holomorphic function in Eq. (3.28) can be evaluated by the method given in Muskhelishvili [12, Chapter4]

$$\frac{1}{\pi}\int_c^d \frac{f(t)}{t-r}dt=\frac{e^{\pi i/2}}{\sin(\pi/2)}\frac{f^*(c)}{\sqrt{(d-c)}}\frac{1}{\sqrt{(r-c)}}-\frac{e^{-\pi i/2}}{\sin(\pi/2)}\frac{f^*(d)}{\sqrt{(d-c)}}\frac{1}{\sqrt{(d-r)}}+F^*(r) \tag{3.31}$$

where $F^*(r)$ is bounded for $(c < r < d)$.

When r approaches c, second part of Eq.(3.31) will be bounded and hence Eq. (3.31) becomes

$$\frac{1}{\pi}\int_c^d \frac{f(t)}{t-r}dt=\frac{f^*(c)}{\sqrt{(d-c)}\sqrt{(c-r)}}+F^{**}(r) \tag{3.32}$$

where $F^{**}(r)$ contains all the bounded terms. Now with Eqs. (3.28) and (3.32), the stress intensity factor given by Eq. (3.26a) can be expressed in terms of the unknown function $f^*(r)$ as

$$k_c=\frac{4\mu}{\kappa+1}\lim_{r\to c}\sqrt{2(c-r)}\frac{f^*(c)}{\sqrt{d-c}\sqrt{c-r}}=\frac{4\mu}{\kappa+1}\frac{f^*(c)}{\sqrt{\frac{d-c}{2}}} \tag{3.33}$$

Comparing Eqs. (3.21) and (3.30) one can relate $f^*(t)$ and $\bar{F}(\tau)$ by

$$f^*(\tau) = \frac{d-c}{2}\bar{F}(\tau) \qquad (-1 < \tau < 1) \tag{3.34}$$

Now substituting Eq. (3.34) into (3.33), the normalized stress intensity factor k`(c) can be obtained

$$k^{'}(c) = \frac{k_c}{p_0\sqrt{\frac{d-c}{2}}} = \frac{4\mu}{p_0(\kappa+1)}\bar{F}(-1) \tag{3.35}$$

and similarly

$$k^{'}(d) = \frac{k_d}{p_0\sqrt{\frac{d-c}{2}}} = -\frac{4\mu}{p_0(\kappa+1)}\bar{F}(1) \tag{3.36}$$

where p_0 is the mean pressure on the crack surfaces.

3.3.2 Stress Intensity Factor for the Case of Crack Terminating at the Rigid Cylinder (a=c<d<b).

In this special case Eq. (3.1) is still valid. However, the kernel is no longer bounded for all values of t and r, and contains point singularities at t=r=a.

Let us assume that $\bar{f}(\tau)$ has the following form

$$\bar{f}(\tau) = \bar{F}(\tau)(1-\tau)^{-\gamma}(1+\tau)^{-\beta}, \qquad (1 > \mathrm{Re}(\gamma,\beta) > 0) \tag{3.37}$$

and the characteristic equations giving γ, β are,

$$\cot(\pi\gamma)=0: \quad \gamma=1/2,$$

$$2\kappa\cos(\pi\beta)+4(\beta-1)^2-(\kappa^2+1)=0. \tag{3.38}$$

The weights C_i in Eqs. (3.23) and (3.26) are the weight of Jacobi polynomials. τ_i and ξ_i are the roots of

$$P_n^{(-\alpha,-\beta)}(\tau_i)=0 \qquad (j=1,...,n) \quad ,$$

$$P_{n-1}^{(1-\alpha,1-\beta)}(\xi_i)=0 \qquad (j=1,...,n-1) \quad . \tag{3.39}$$

Following the procedure described in [4] and a similar procedure followed in the previous section, k´(c) and k´(d) can be computed as,

$$k^{'}(c)=\frac{k_a}{p_0\left(\frac{d-c}{2}\right)^{\beta}}=\frac{4\mu}{p_0(\kappa+1)}q\,\overline{F}(-1) \quad ,$$

$$k^{'}(d)=\frac{k_d}{p_0\sqrt{\frac{d-c}{2}}}=-\frac{4\mu}{p_0(\kappa+1)}2^{1/2-\beta}\overline{F}(1) \quad , \tag{3.40}$$

where

$$k_a=\lim_{r\to a}\sqrt{2}\,(a-r)^{\beta}\,\sigma_z(r,0),$$

$$q=(\kappa+1)\left[(1-2\beta)/\kappa+2\beta-3\right]/2\sin(\pi\beta). \tag{3.41a, b}$$

3.3.3 Stress Intensity Factor for the Case of External Edge Crack (a<c<d=b).

Following a similar procedure as in section 3.3.1, one can obtain

$$k_c=\lim_{r\to c}\sqrt{2(c-r)}\sigma_z(r,0),$$

$$k^{'}(c)=\frac{k_c}{p_0\sqrt{d-c}}=\frac{4\mu}{p_0(\kappa+1)}\overline{F}(-1) \tag{3.42}$$

CHAPTER IV

NUMERICAL RESULTS AND CONCLUSIONS

In this study, Poisson's ratio is used as the material parameter and the ratios of the inner radius of the annulus, outer and inner radii of the crack to the outer radius of the annulus are used as the geometric parameters. The numerical results are presented in graphical form. These results are obtained for three different loading conditions on crack surfaces.

$$P_1(r) = p_0,$$

$$P_2(r) = \frac{3\,(d^2 - c^2)(r-a)}{2d^3 - 3ad^2 - 2c^3 + 3ac^2}\, p_0,$$

$$P_3(r) = \frac{6\,(d^2 - c^2)(r-a)^2}{3d^4 - 8ad^3 + 6a^2d^2 - 3c^4 + 8ac^3 - 6a^2c^2}\, p_0, \tag{4.1}$$

where p_0 is the mean compressive load on the crack surfaces.

Introducing the dimensionless geometrical parameters

$$r_1 = \frac{a}{b}, \quad r_2 = \frac{c}{b} \text{ and } r_3 = \frac{d}{b}, \tag{4.2}$$

$$\overline{P}_1(\xi) = p_0,$$

$$\overline{P}_2(\xi) = \frac{3\,(r_3^{\,2} - r_2^{\,2})\left[(r_3 - r_2)\xi + r_3 + r_2 - 2r_1\right]}{2(2r_3^{\,3} - 3r_1r_3^{\,2} - 2r_2^{\,3} + 3r_1r_2^{\,2})}\, p_0,$$

$$\overline{P}_3(\xi) = \frac{3\,(r_3^{\,2} - r_2^{\,2})\left[(r_3 - r_2)\xi + r_3 + r_2 - 2r_1\right]^2}{2(3r_3^{\,4} - 8r_1r_3^{\,3} + 6r_1^{\,2}r_3^{\,2} - 3r_2^{\,4} + 8r_1r_2^{\,3} - 6r_1^{\,2}r_2^{\,2})}\, p_0 \tag{4.3}$$

are obtained.

Together with the results of this study, results of Birinci [11] in Figure 3 and Geçit [4] in Figure 4 are presented for comparison purposes. As can be observed from Figure 3, results of the present study and results of Birinci are coinciding. In the study of Geçit, a cracked elastic strip bonded to rigid support is considered. When the rigid cylinder approaches the external surface of the annulus (i.e., when a/(b-a)= 100), present study turns out to be the problem studied by Geçit. Figure 4 indicates a similar results when a/(b-a)= 100. Another observation from this figure is that when (b-a) is fixed and a, c→ 0, k`(c) approaches infinity for an external edge crack.

Figures 5-18 show the variation of normalized stress intensity factors k´(c) and k´(d) at the edges of the embedded crack. As may be observed from these figures, k´(c) and k´(d) increase when ν increases or a/b decreases. As can be seen from Figure 9 and 16, as the crack width is fixed and d→b, k`(c) first increases rapidly, then continues to increase slightly, finally increases rapidly again as d increases further. On the other hand, under the same conditions k´(d) first increases slightly, then increases rapidly as crack d increases further. Since crack gets further from the rigid cylinder. As expected, when c→d, k´(c) and k´(d) approach unity. Another observation from Figure 5 and 6 is that when c/b=0.35, a/b=0.25 and crack width gets wider, initially k´(c) and k´(d) reduce slightly, then both of them increase rapidly. k´(c) and k´(d) seem to be slightly effected when crack length has relatively small values. On the other hand, when a/b=0.75 and c/b=0.80 and d/b increases, initially k´(c) reduces considerably more than k´(d), then both of them increase. Further more, as d→b, k`(d) is unbounded whereas k`(c) has finite value. When d/b is fixed and c/b decrease, both k´(c) and k´(d) initially increase, then decrease. This is expected, when crack tip gets closer to rigid cylinder, the rigid cylinder is more effective parameter on k´(c) and k´(d) than the crack length. At this point, one can say that normalized stress intensity factors reduce when crack gets closer to rigid cylinder or crack length gets closer or ν decrease.

From Figures 19-21, it may be seen that when ν decreases or crack length increases k`(c) increases for an external edge crack. When crack length is very small, k`(c) is 1.586. This is expected, since in this case, the stress intensity factors for thick-walled cylinder and for a strip are the same. This value is calculated for a strip problem in [4] and for a thick-walled cylinder in [8].

Figures 22-27 show the variation of the normalized stress intensity factors k´(c) and k´(d) at the edges of the crack terminating at the rigid cylinder. When ν increases, k´(c) reduces, whereas k´(d) increases. There is a rapid change in k´(d) when crack length increases. On the other hand, k´(c) increases slightly. This may occur because of the rigid cylinder.

Three different loading conditions are compared in Figures 28-32. For all conditions $P_1(r), P_2(r)$, and $P_3(r)$ show similar behaviors. One can observe from these figures that when $P(d)/P(c)$ gets greater, k´(c) decreases whereas k´(d) increases for an embedded crack and a crack terminating at the rigid cylinder. Figure 30 shows that when $P(d)/P(c)$ gets greater, k´(c) increases for an external edge crack.

This problem can be solved by using finite element methods, ANSYS, MARC and experimentally as a further studies.

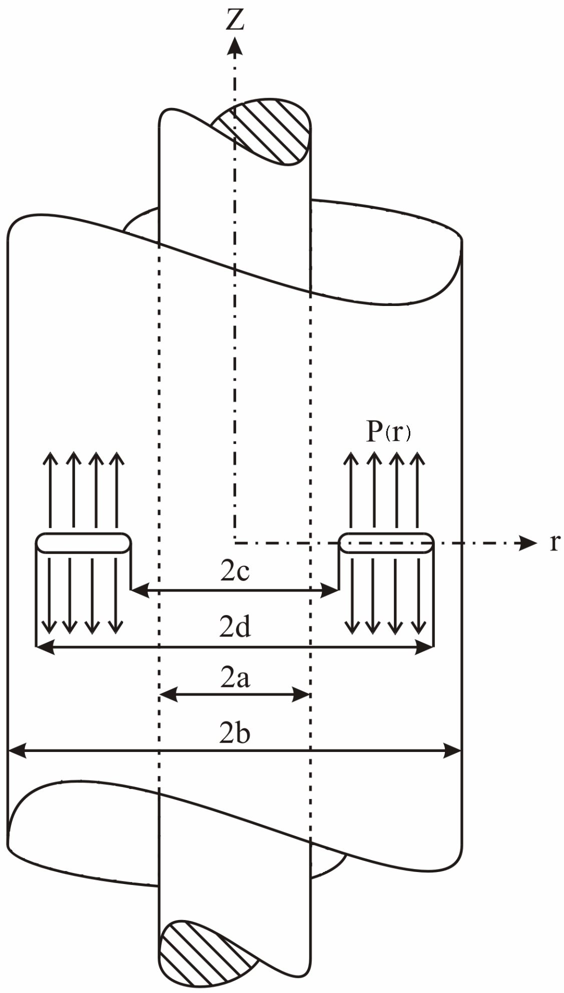

Figure 1. Geometry of the infinite annulus bonded to rigid cylinder.

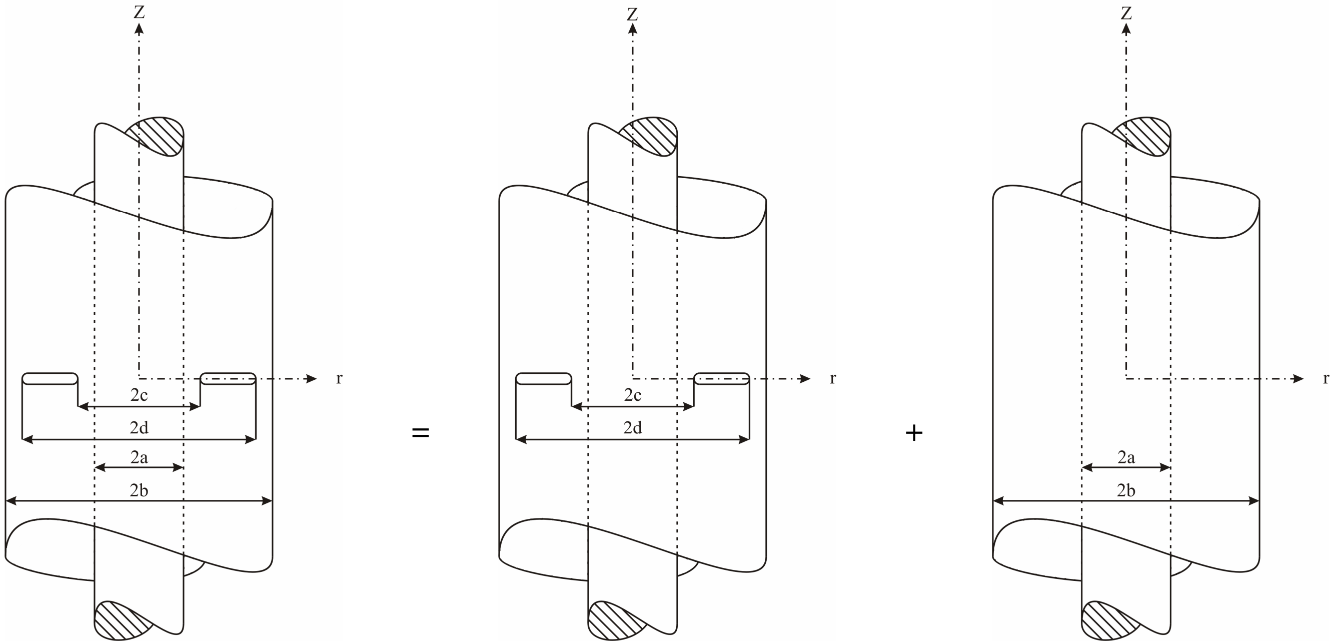

(i)
Hankel transform
in r-direction

(ii)
Fourier transform
in z-direction

Figure 2. The informal superposition scheme (Perturbation problem).

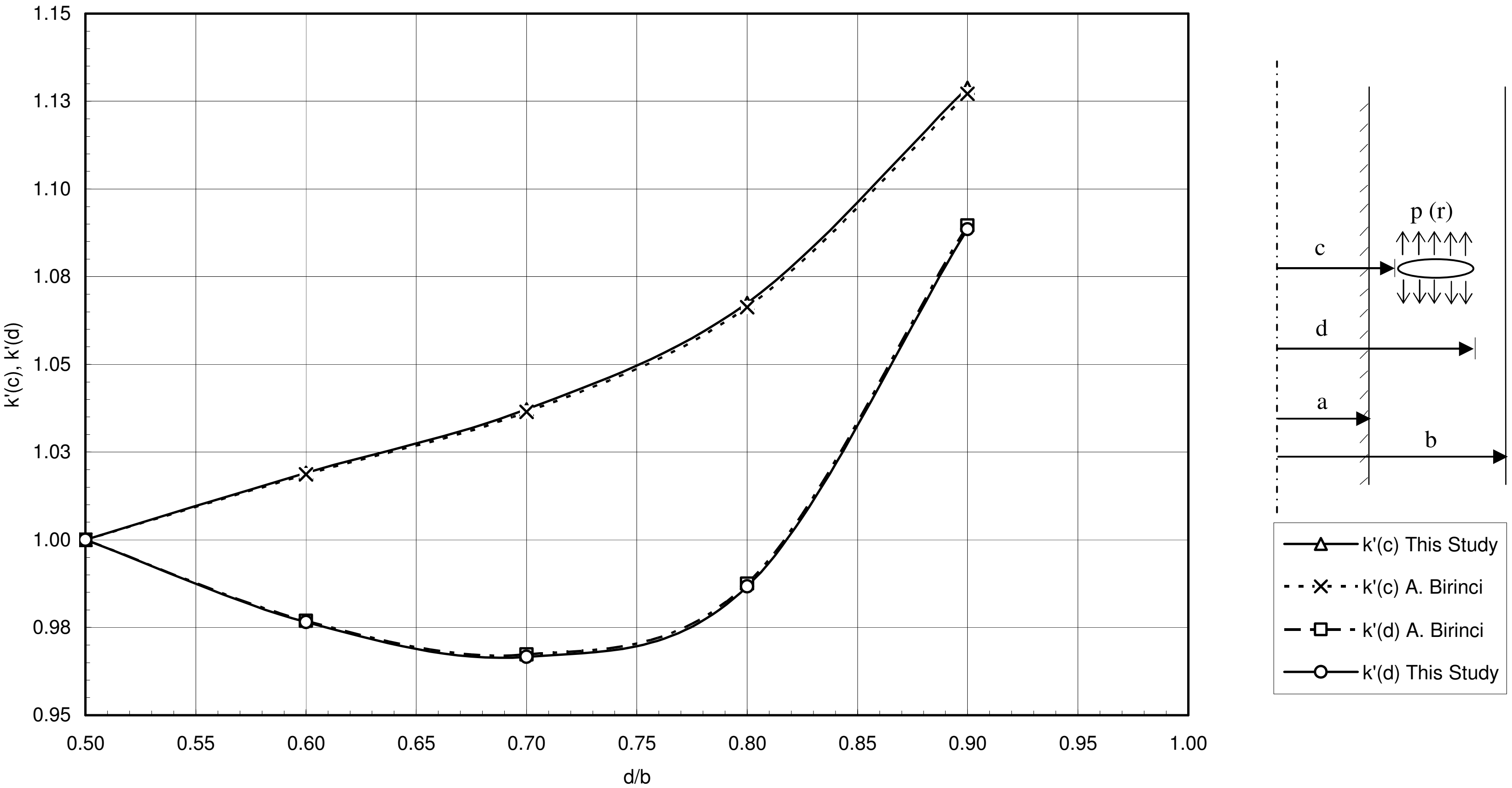

Figure 3. Comparison of results obtained in this study with A. Birinci [11] (ν=0.30, a/b=0.30, c/b=0.50).

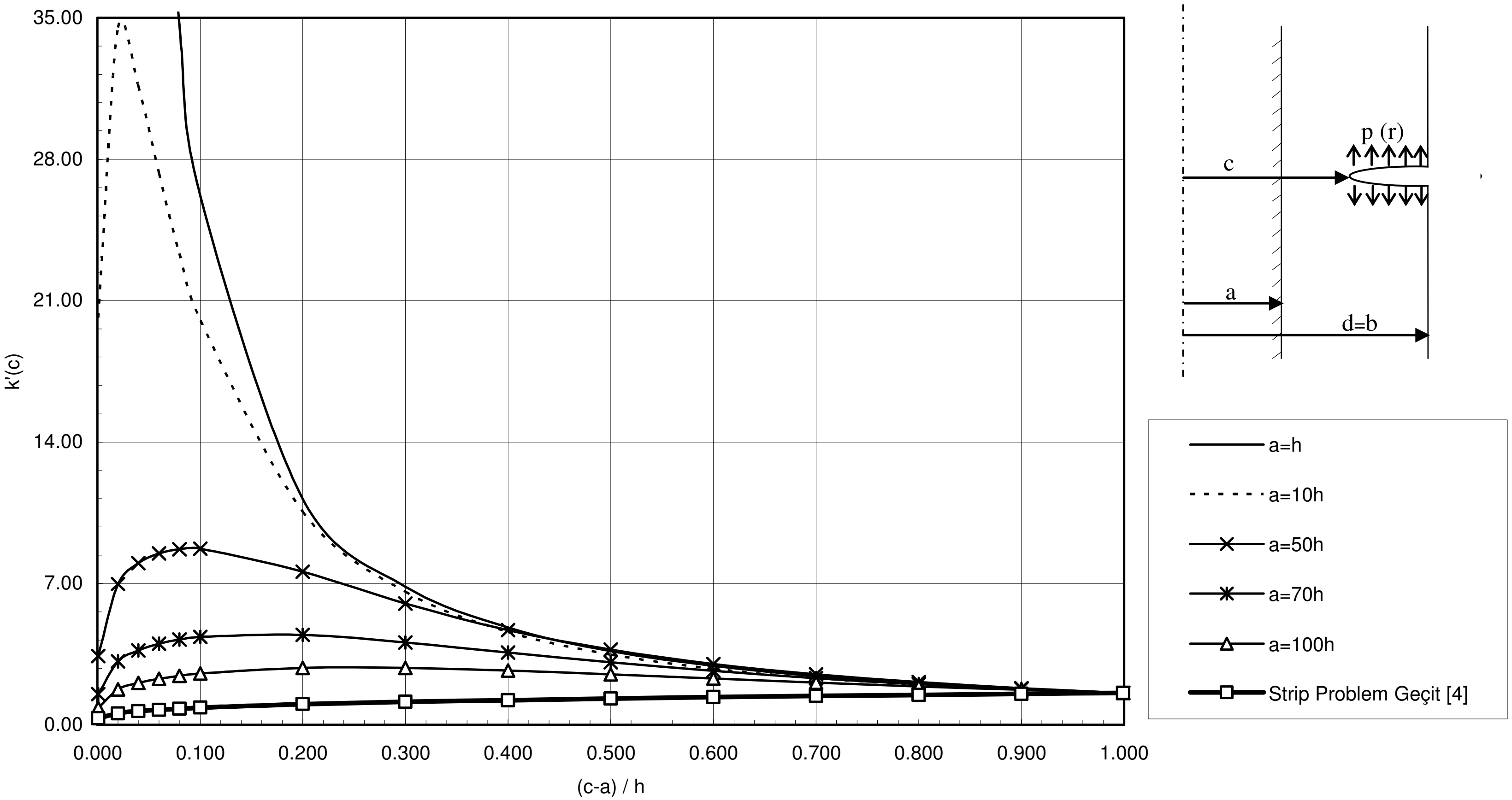

Figure 4. Comparison of results obtained in this study with M.R. Geçit [4] (ν=0.25, h=b-a, d/b=1.0).

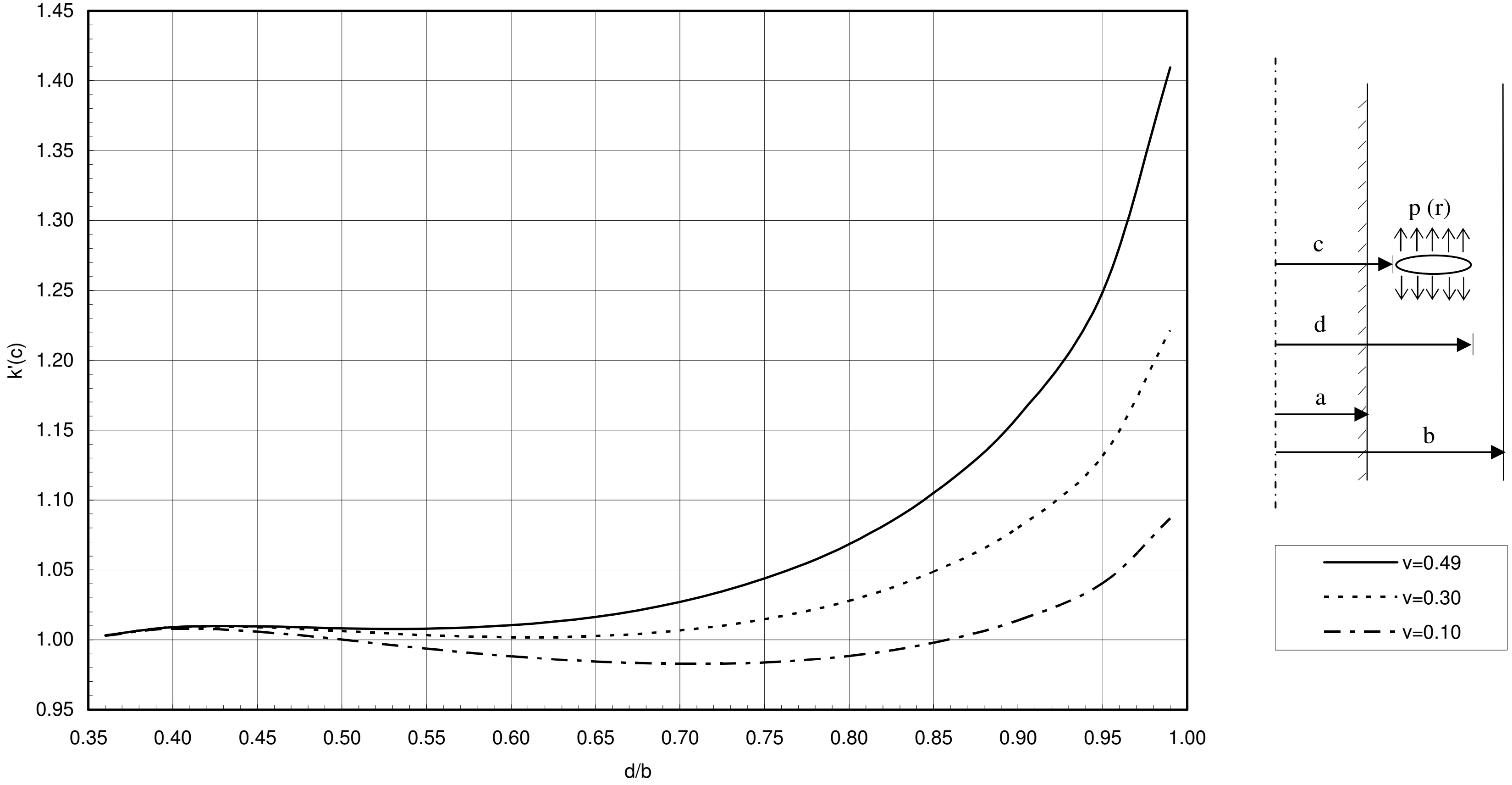

Figure 5. Variation of stress intensity factor k'(c) with d/b and ν for an embedded crack (a/b=0.25, c/b=0.35).

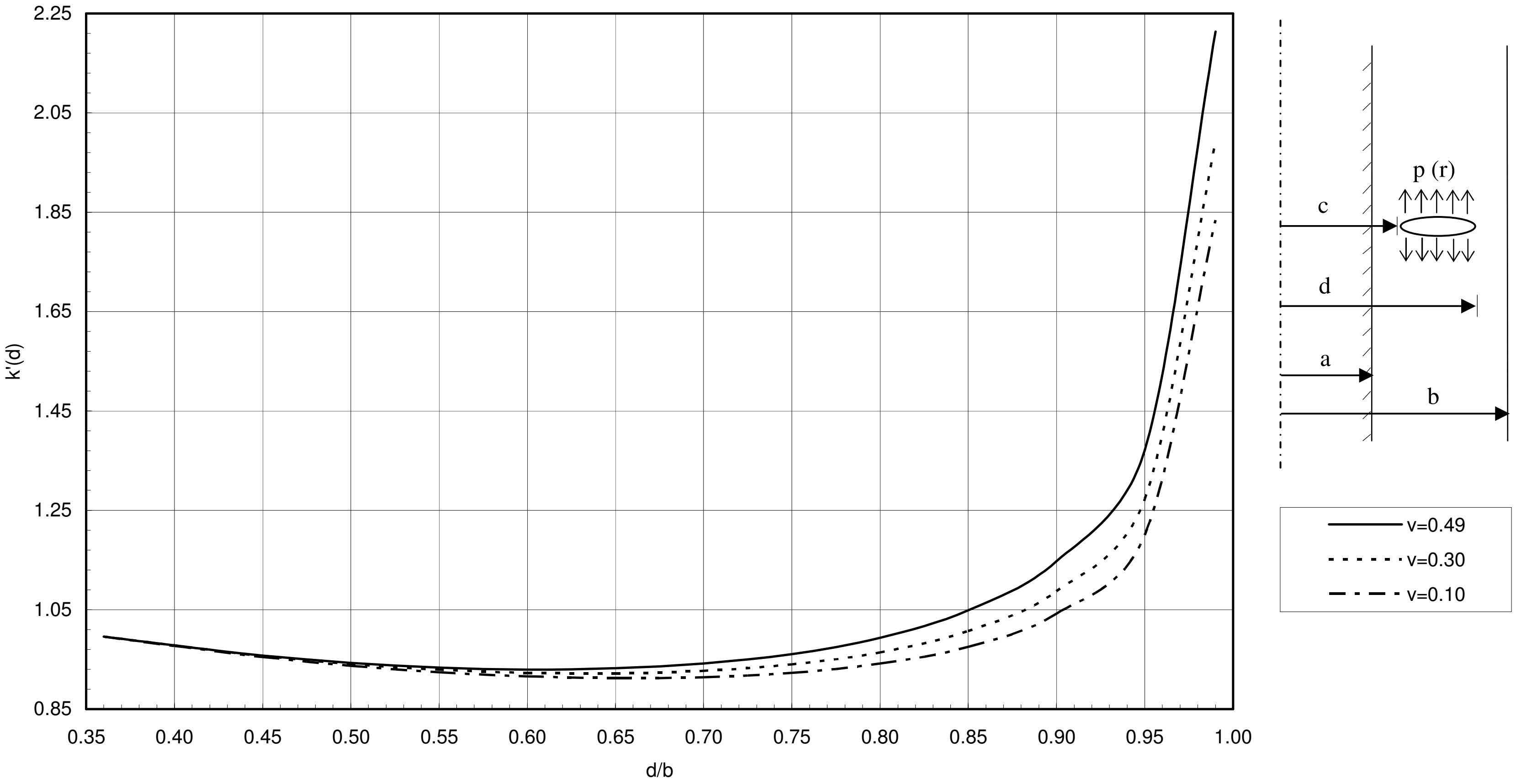

Figure 6. Variation of stress intensity factor k’(d) with d/b and ν for an embedded crack (a/b=0.25, c/b=0.35).

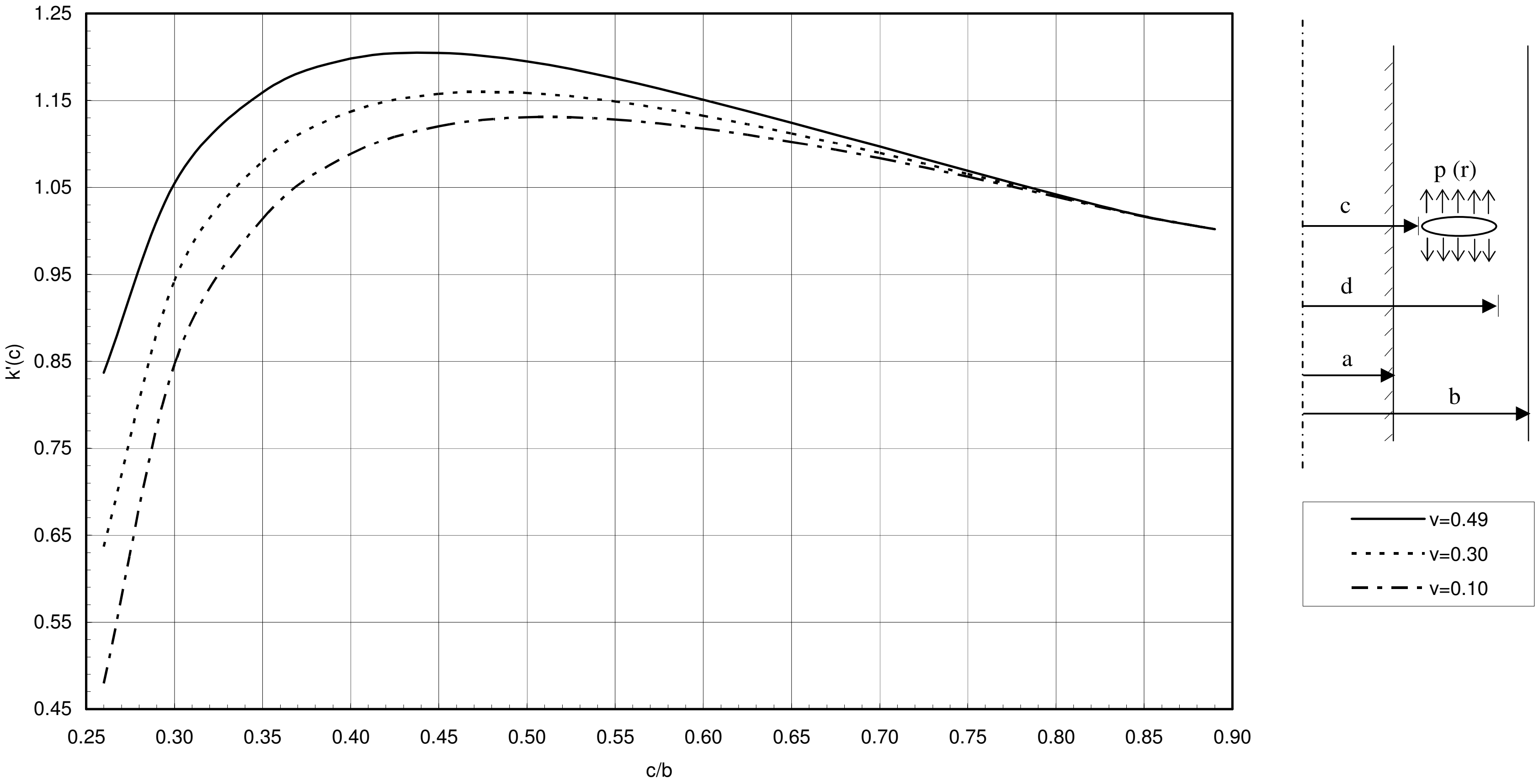

Figure 7. Variation of stress intensity factor k'(c) with c/b and ν for an embedded crack (a/b=0.25, d/b=0.90).

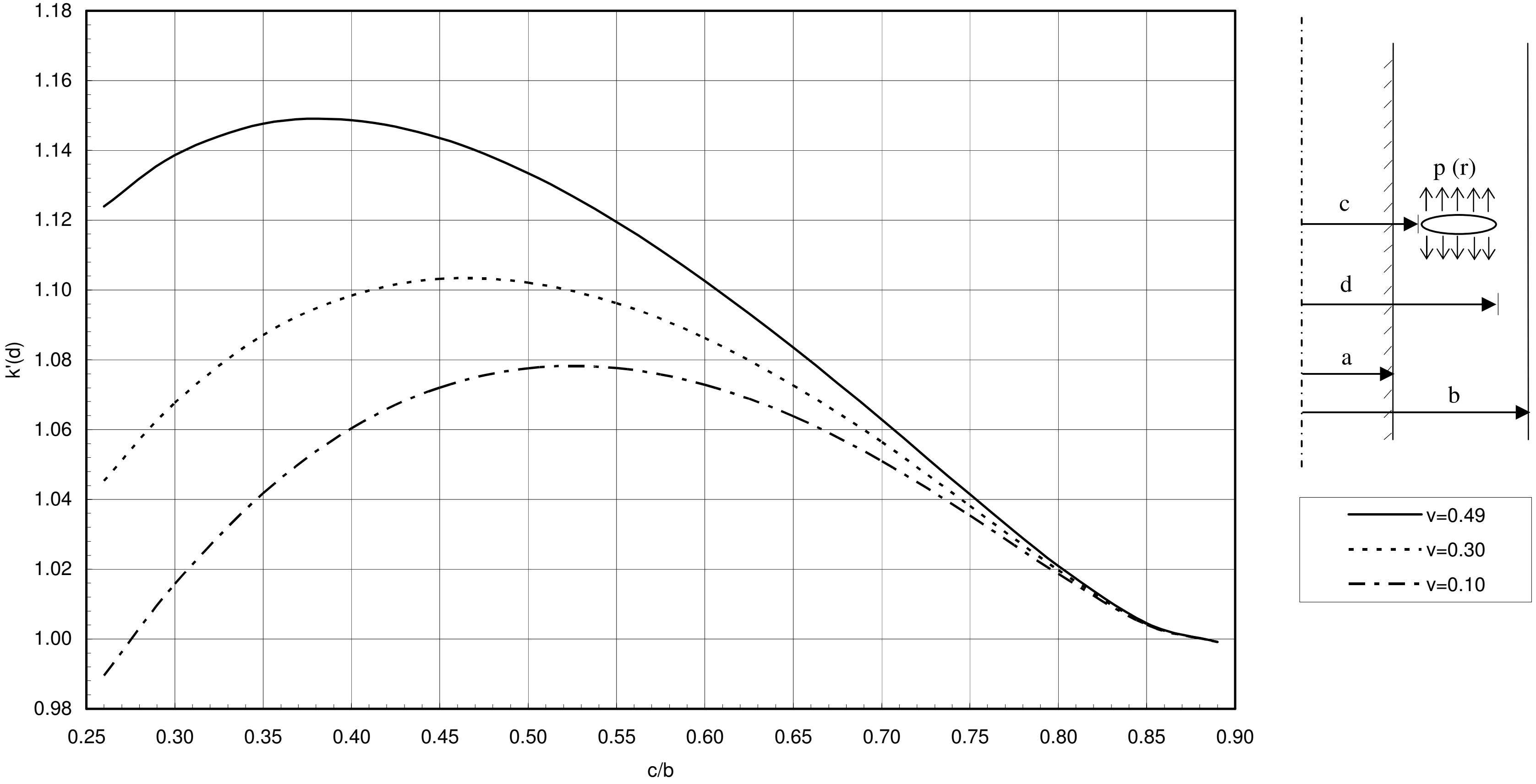

Figure 8. Variation of stress intensity factor k'(d) with c/b and ν for an embedded crack (a/b=0.25, d/b=0.90).

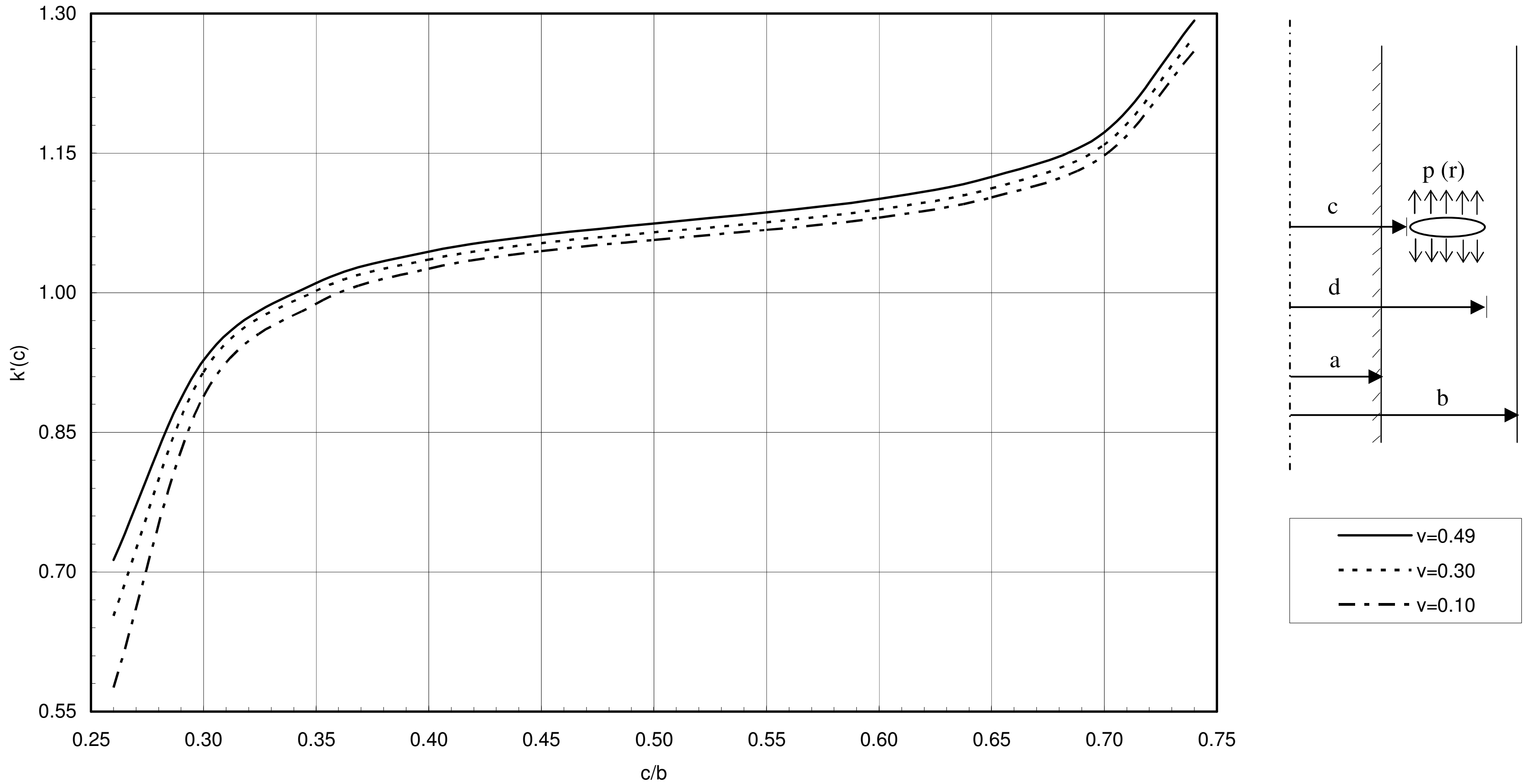

Figure 9. Variation of stress intensity factor k'(c) with c/b and ν for an embedded crack (a/b=0.25, (d-c)/b=0.25).

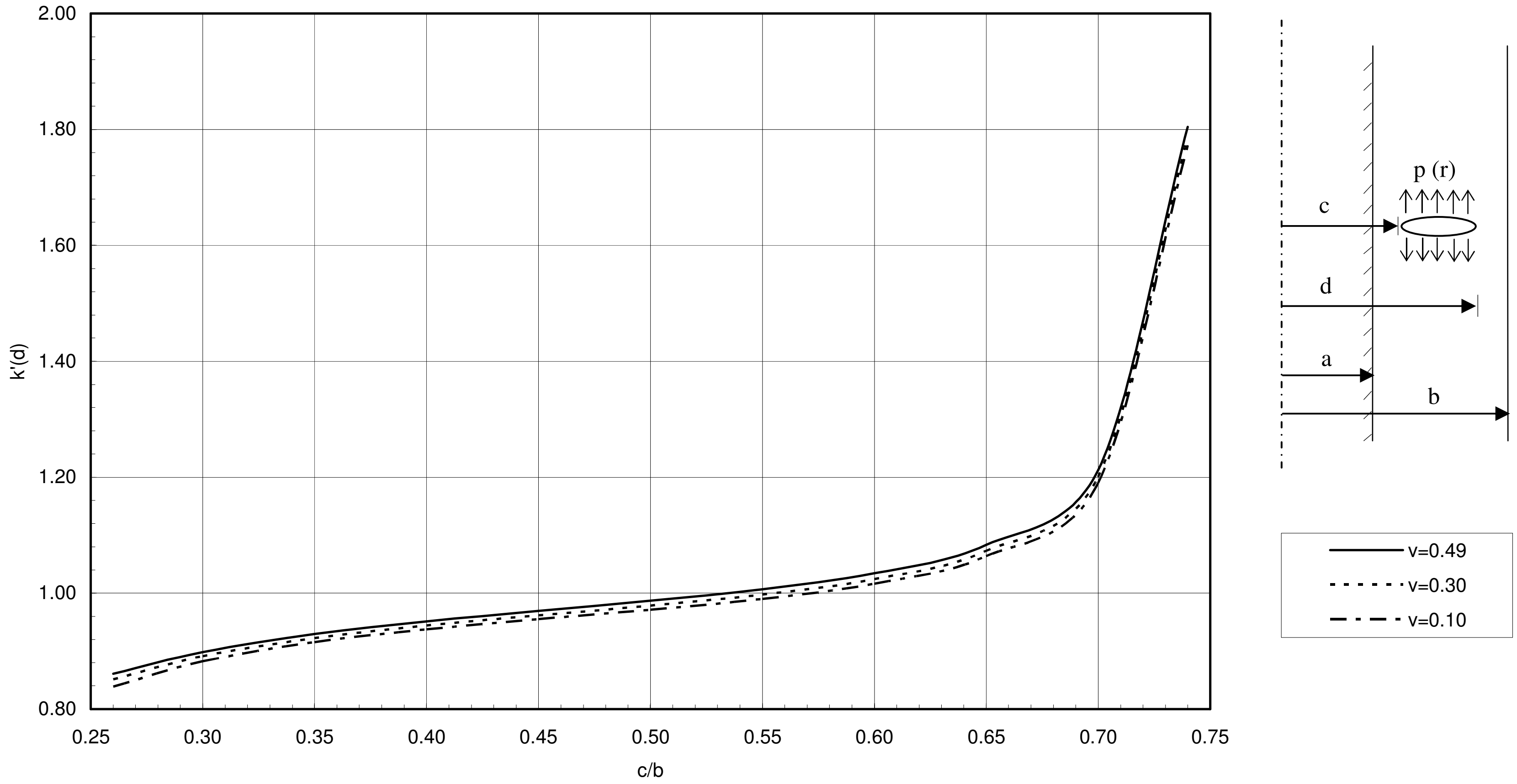

Figure 10. Variation of stress intensity factor k'(d) with c/b and ν for an embedded crack (a/b=0.25, (d-c)/b=0.25).

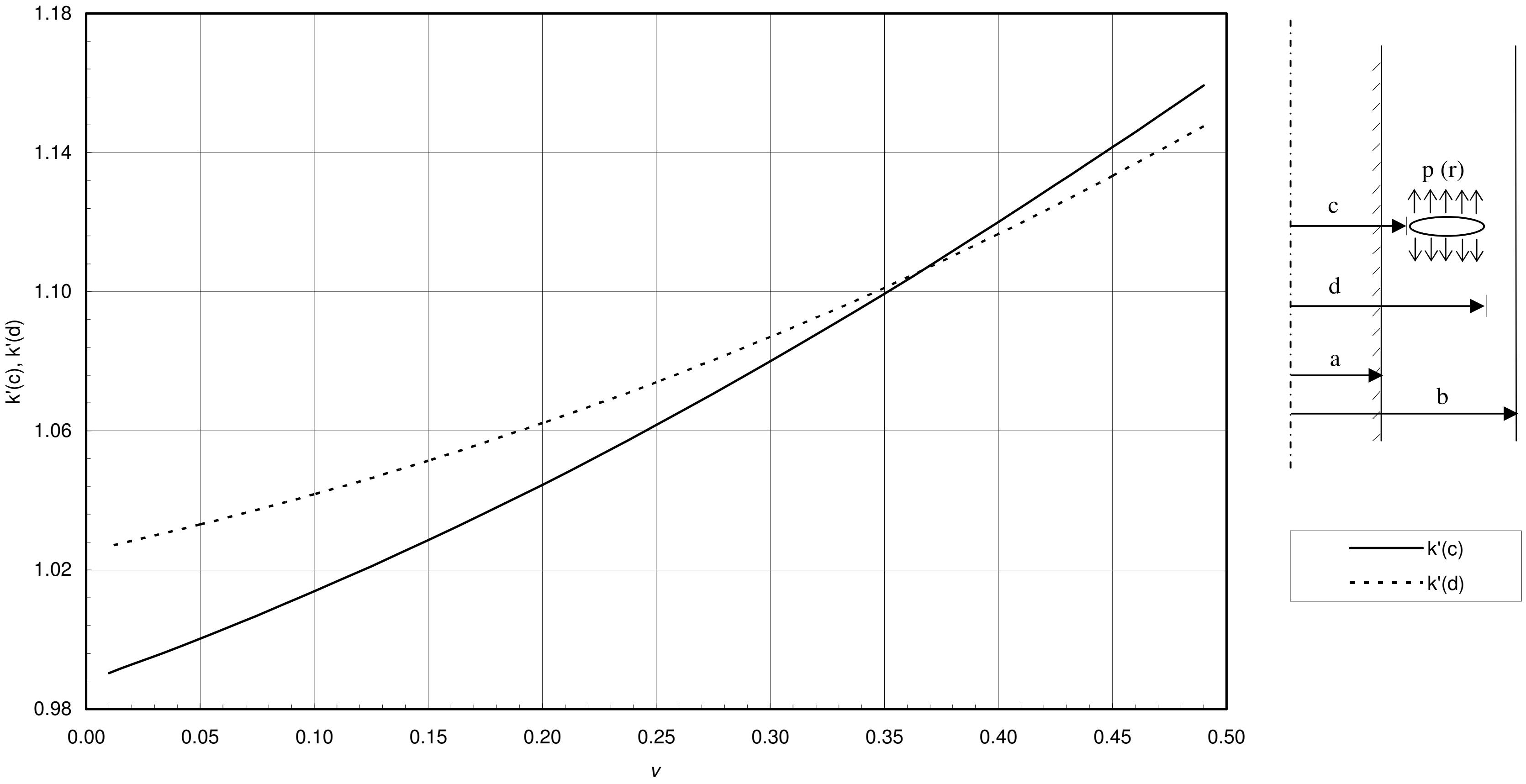

Figure 11. Variation of stress intensity factor k'(c), k'(d) with ν for an embedded crack (a/b=0.25, c/b=0.35, d/b=0.90).

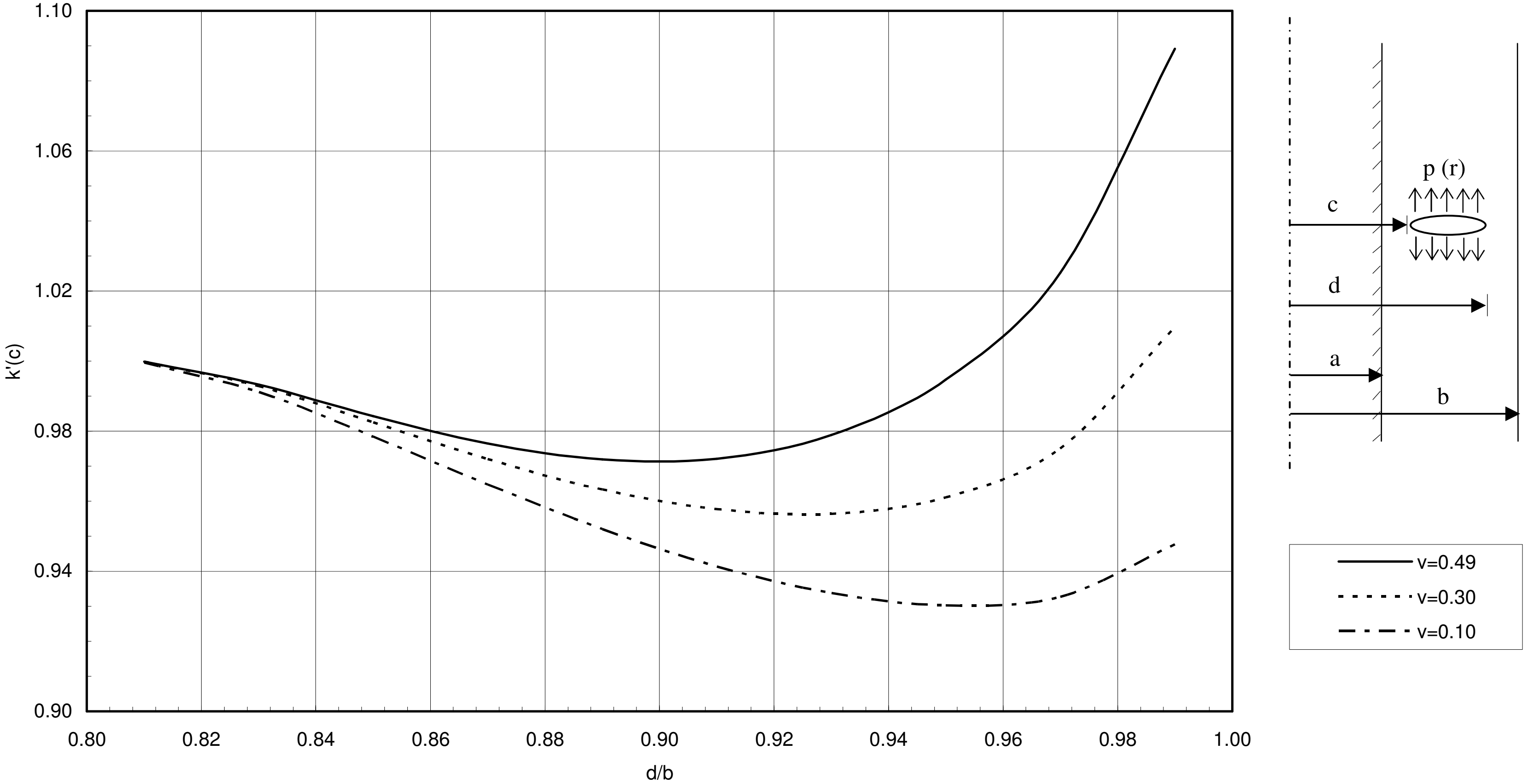

Figure 12. Variation of stress intensity factor k'(c) with d/b and ν for an embedded crack (a/b=0.75, c/b=0.80).

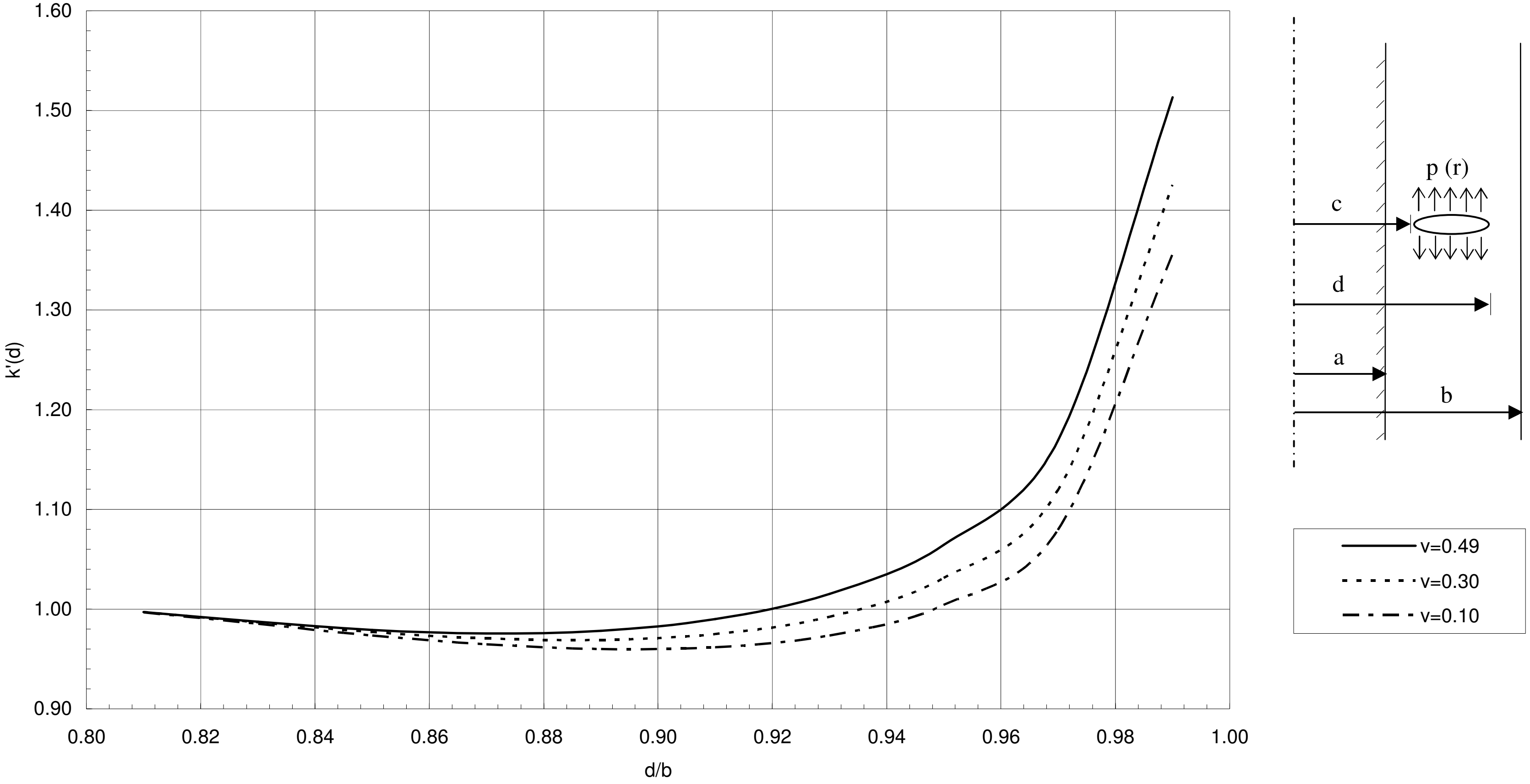

Figure 13. Variation of stress intensity factor k'(d) with d/b and ν for an embedded crack (a/b=0.75, c/b=0.80).

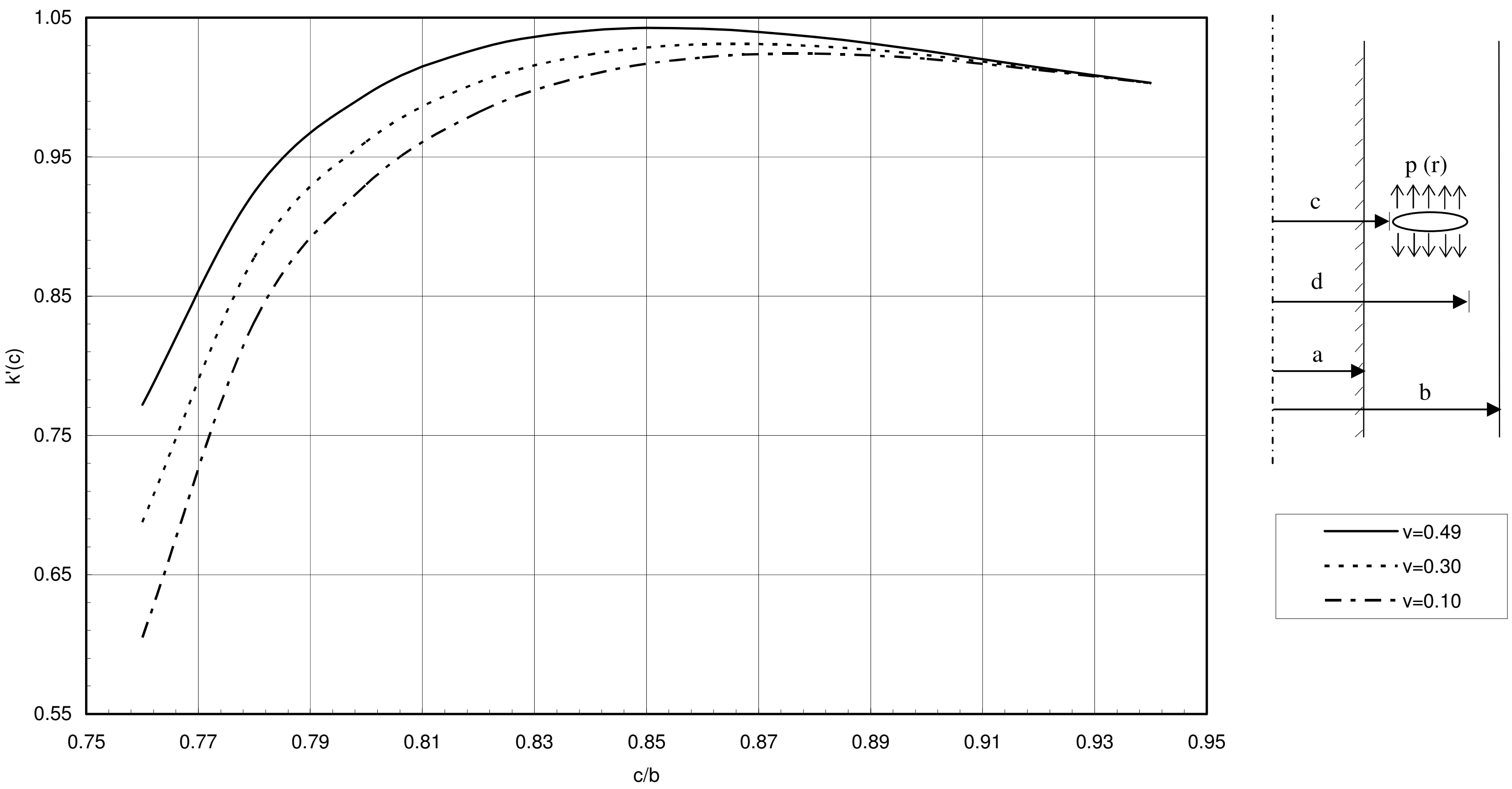

Figure 14. Variation of stress intensity factor k'(c) with c/b and ν for an embedded crack (a/b=0.75, d/b=0.95).

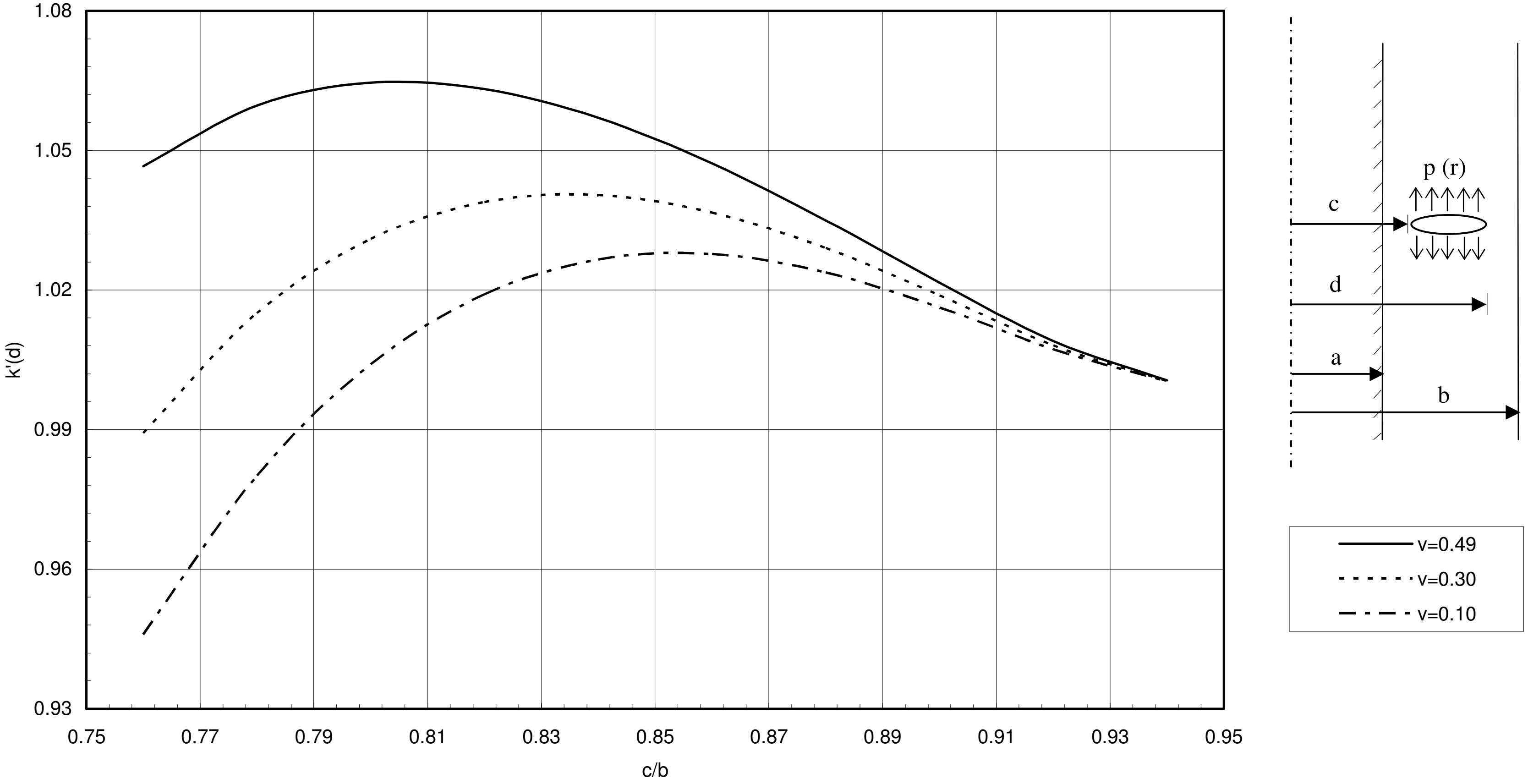

Figure 15. Variation of stress intensity factor k'(d) with c/b and ν for an embedded crack (a/b=0.75, d/b=0.95).

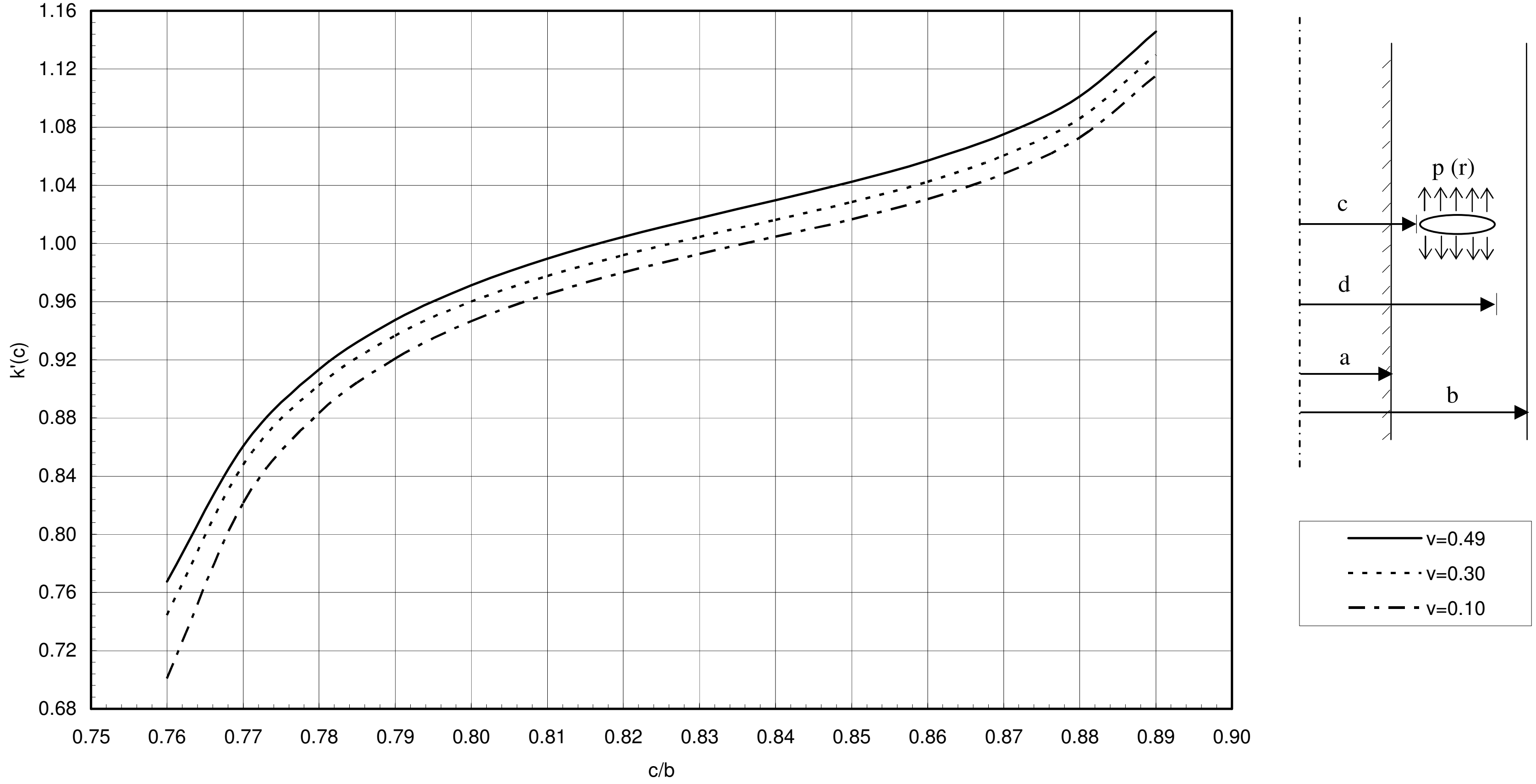

Figure 16. Variation of stress intensity factor k'(c) with c/b and ν for an embedded crack (a/b=0.75, (c-d)/b=0.10).

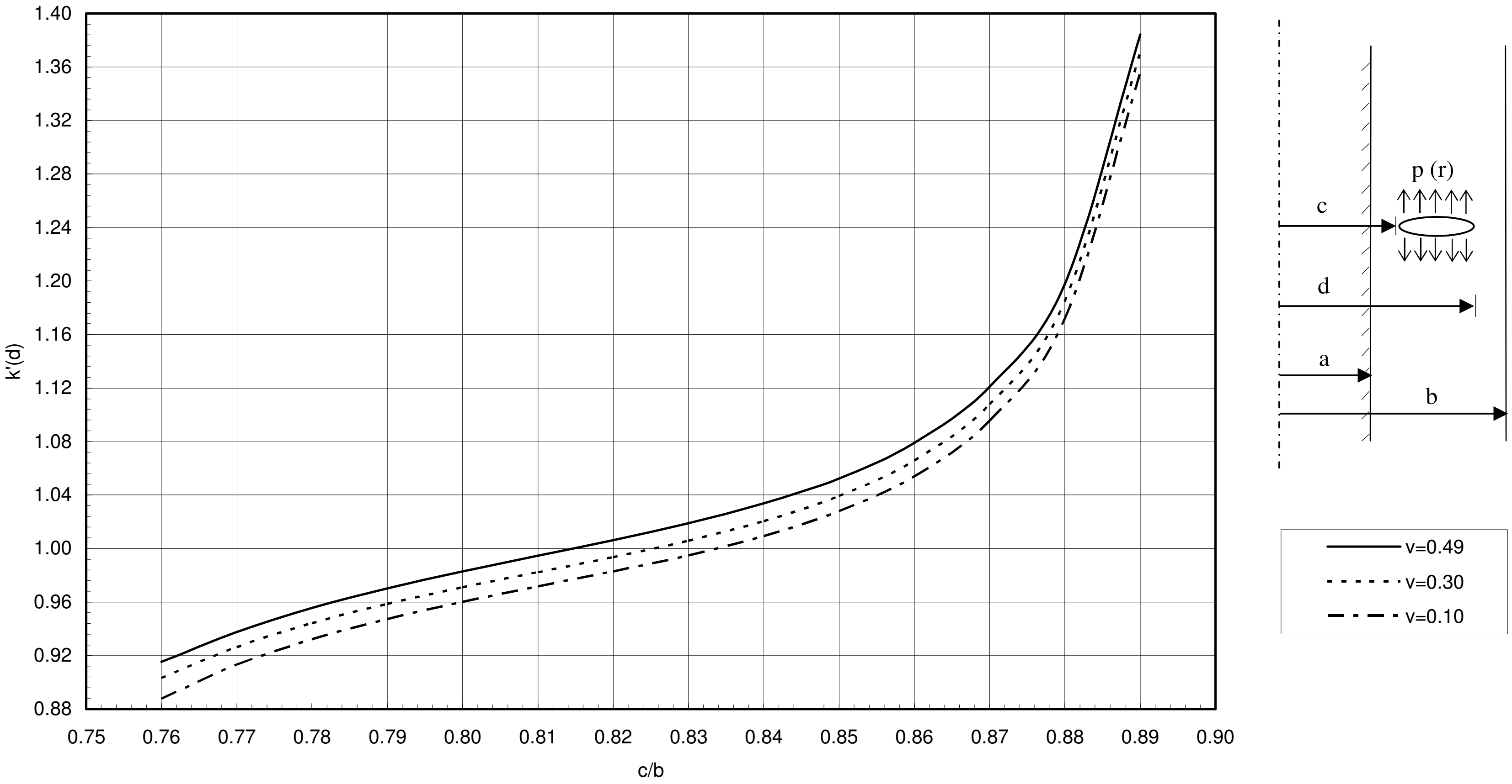

Figure 17. Variation of stress intensity factor k'(d) with c/b and ν for an embedded crack (a/b=0.75, (c-d)/b=0.10).

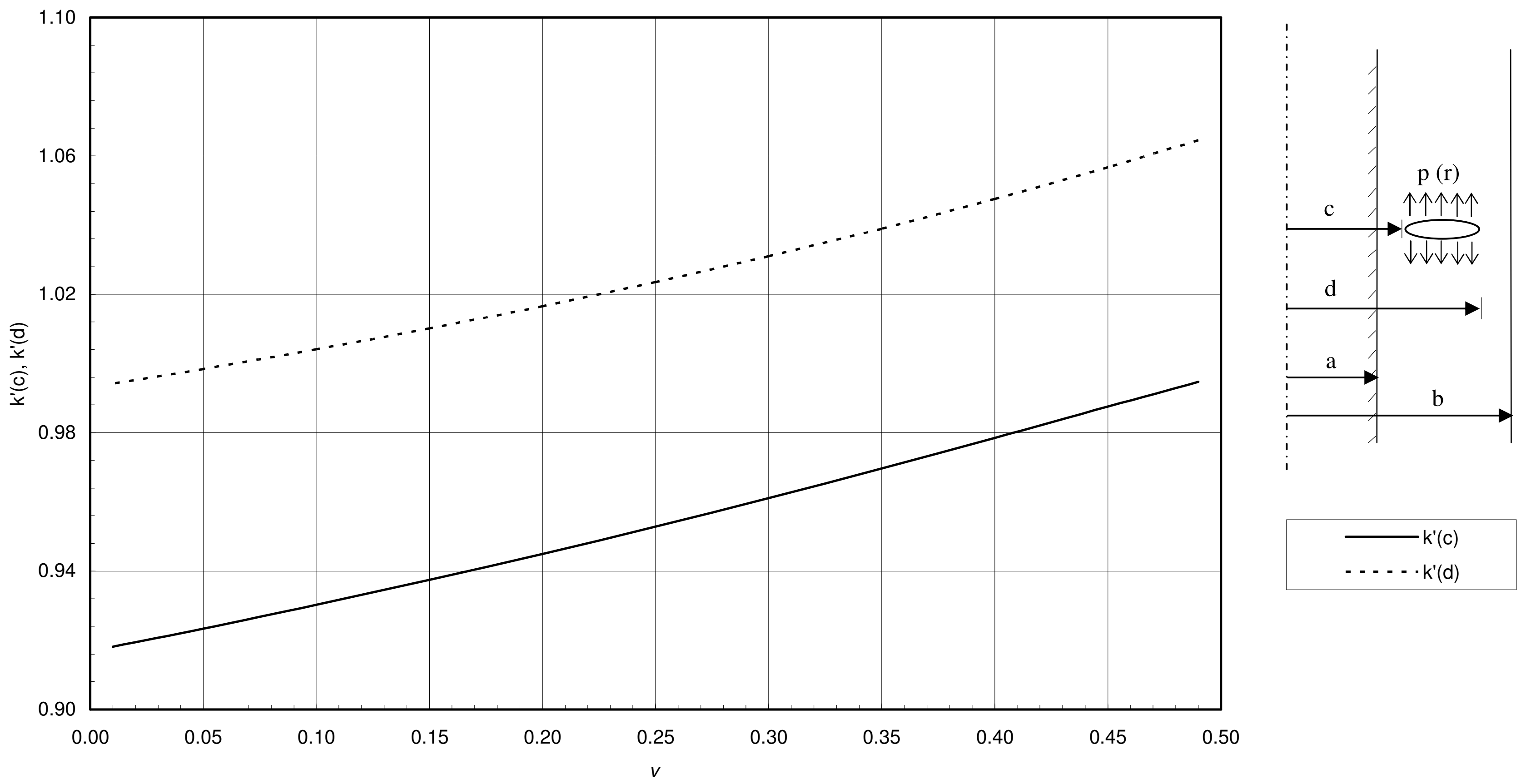

Figure 18. Variation of stress intensity factor k'(c), k'(d) with ν for an embedded crack (a/b=0.75, c/b=0.80, d/b=0.95).

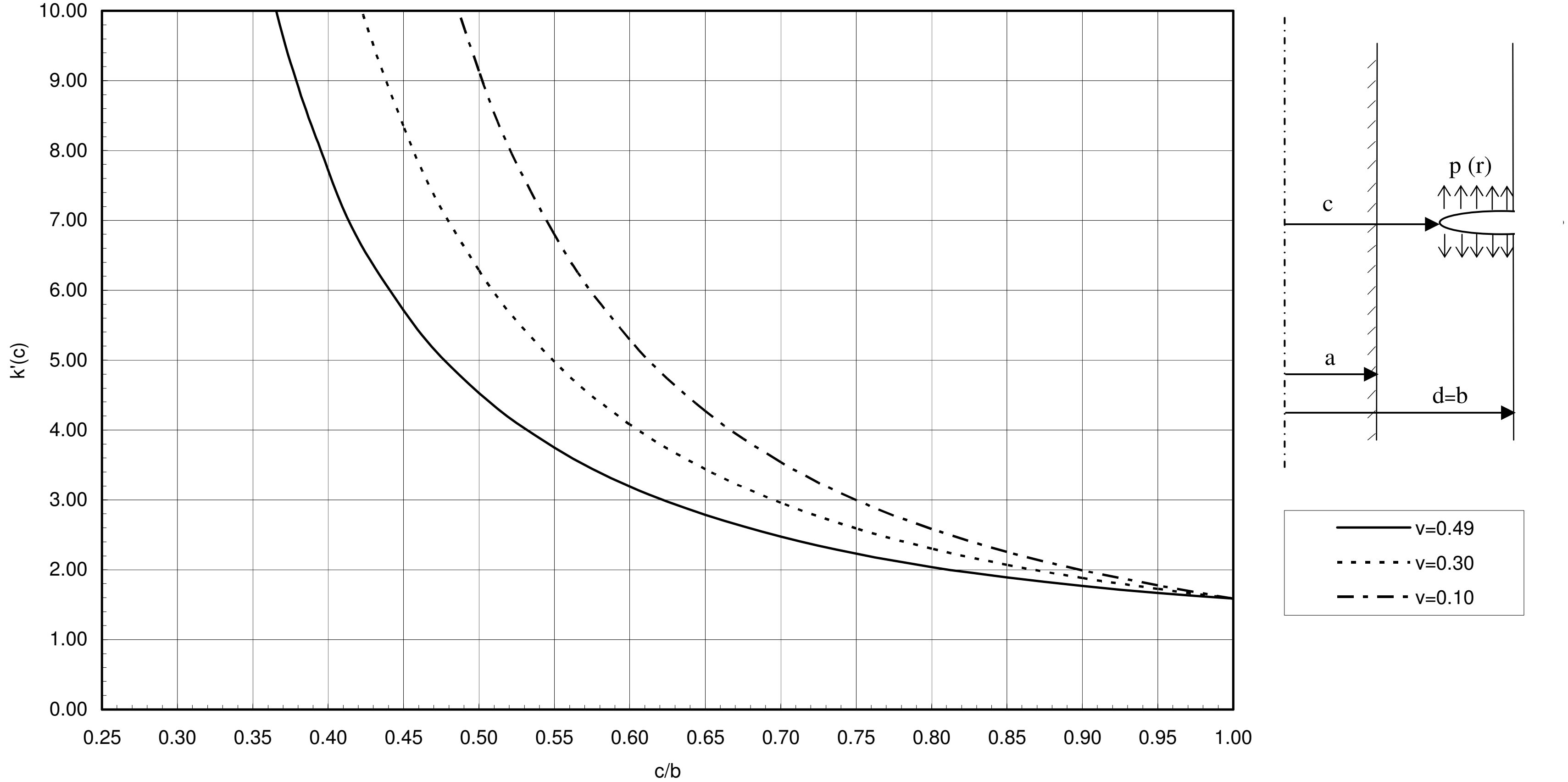

Figure 19. Variation of stress intensity factor k'(c) with c/b and ν for an external edge crack (a/b=0.25, d/b=1.0).

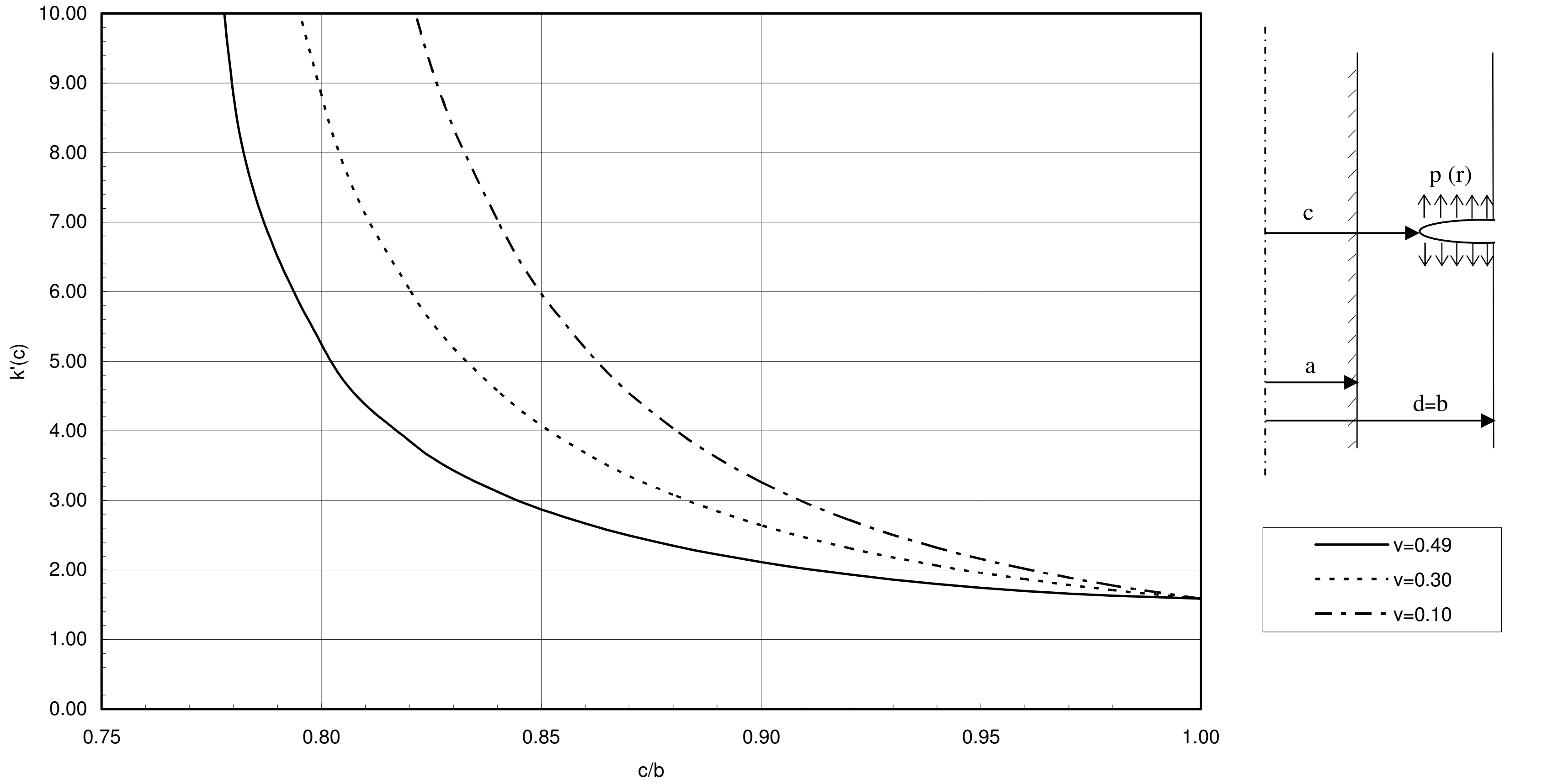

Figure 20. Variation of stress intensity factor k’(c) with c/b and ν for an external edge crack (a/b=0.25, d/b=1.0).

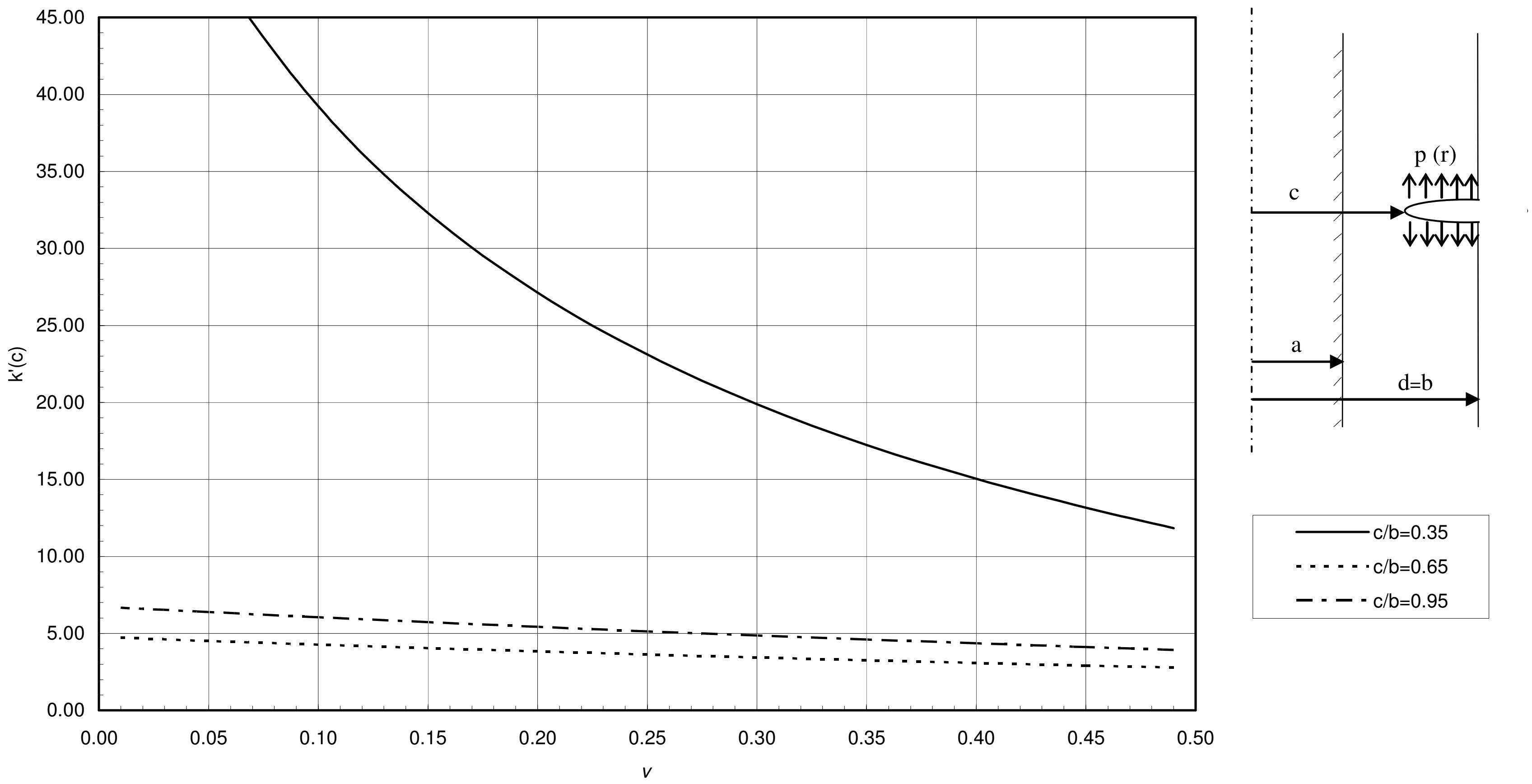

Figure 21. Variation of stress intensity factor k'(c) with ν for an external edge crack (a/b=0.25, c/b=0.35 d/b=1.0).

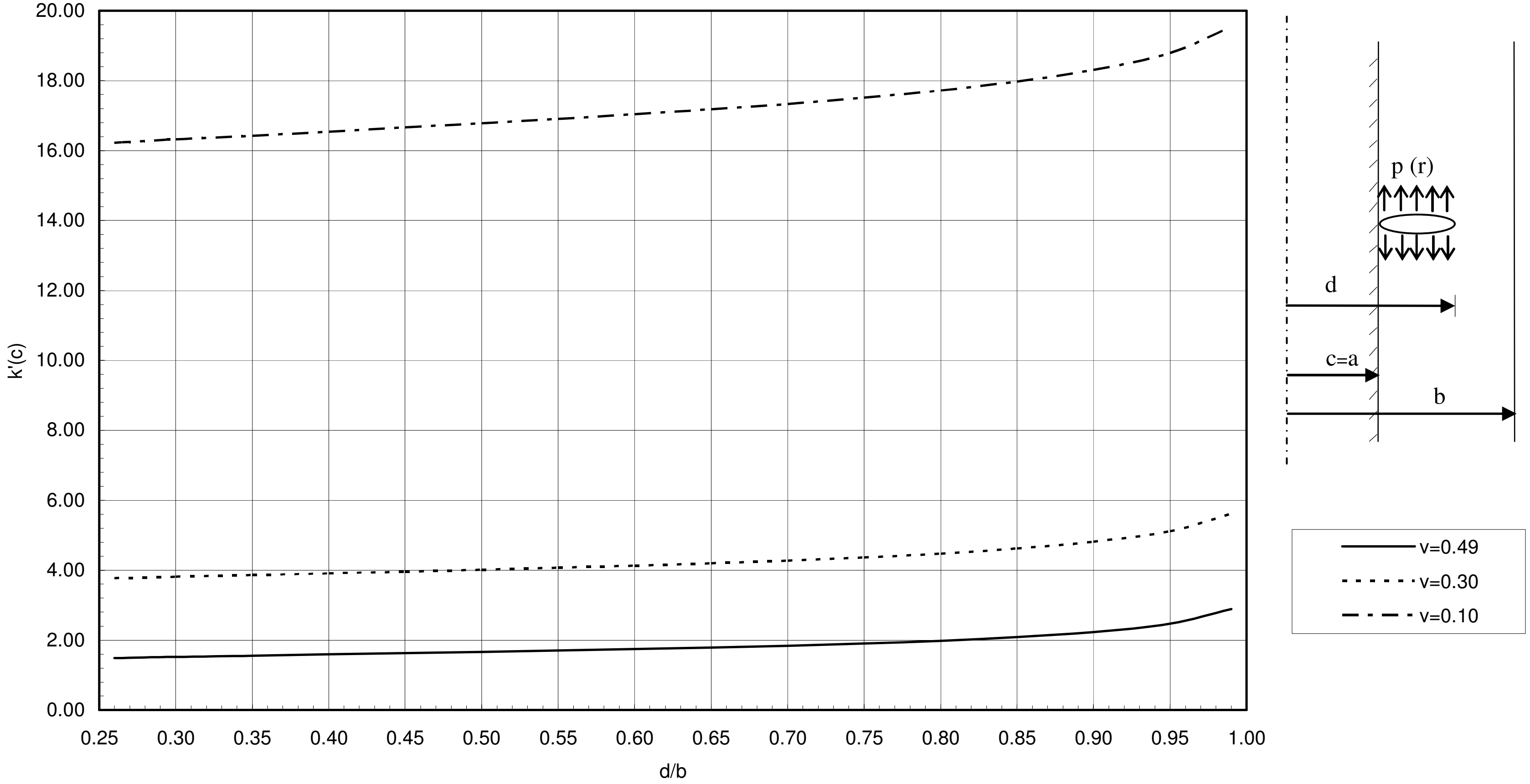

Figure 22. Variation of stress intensity factor k'(c) with d/b and ν for a crack terminating at the rigid cylinder (a/b=c/b=0.25).

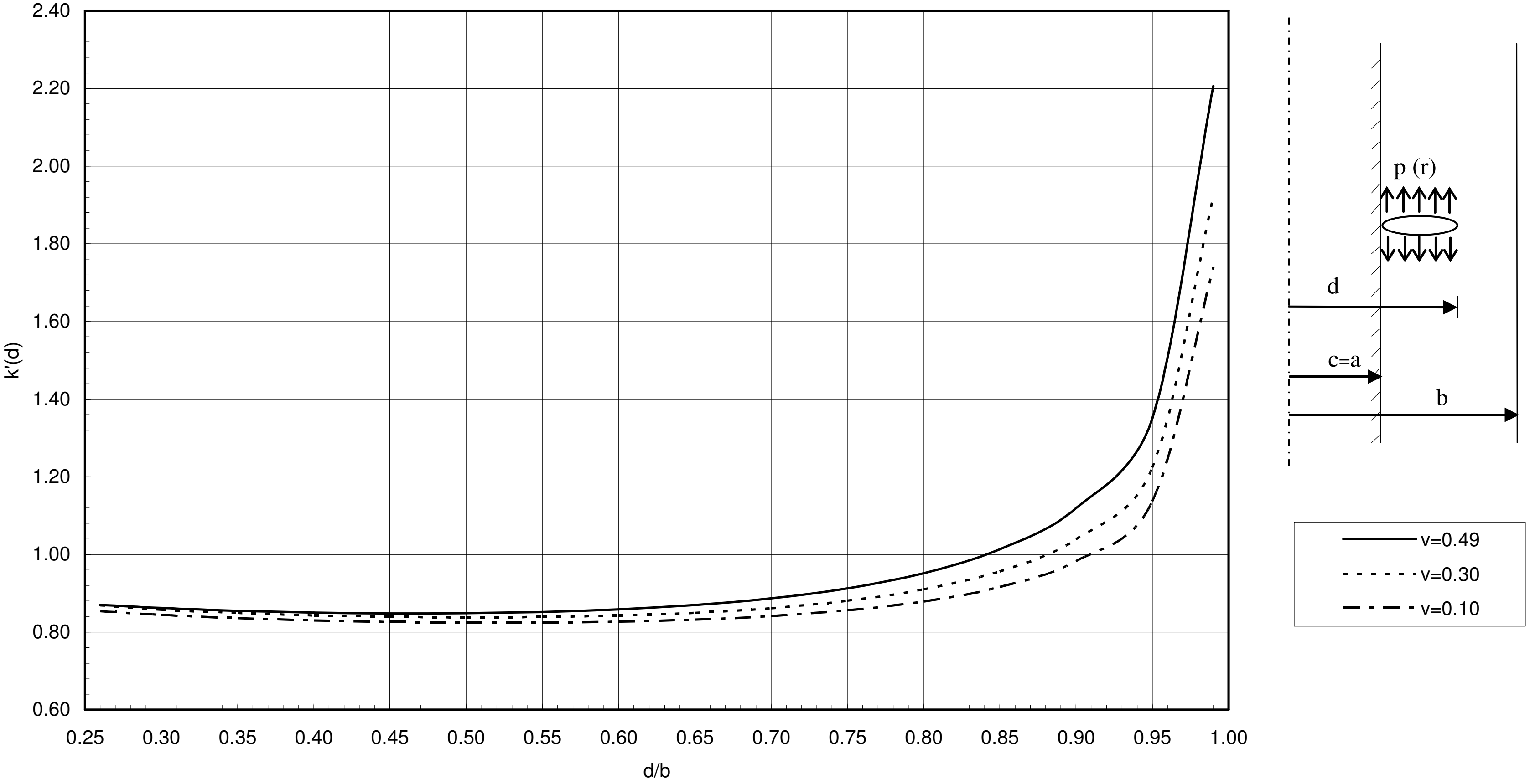

Figure 23. Variation of stress intensity factor k'(d) with c/b and ν for a crack terminating at the rigid cylinder (a/b=c/b=0.25).

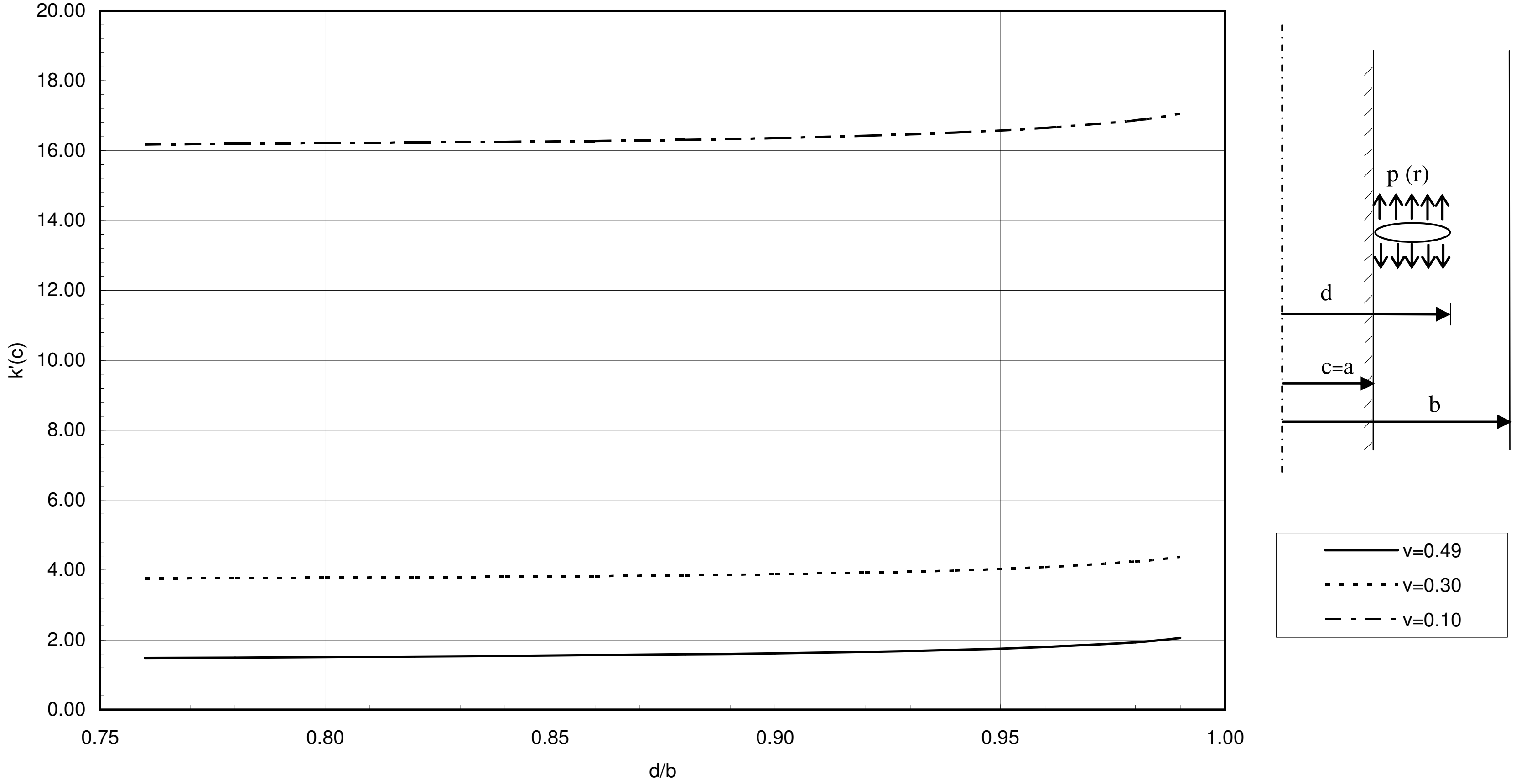

Figure 24. Variation of stress intensity factor k'(c) with c/b and ν for a crack terminating at the rigid cylinder (a/b=c/b=0.75).

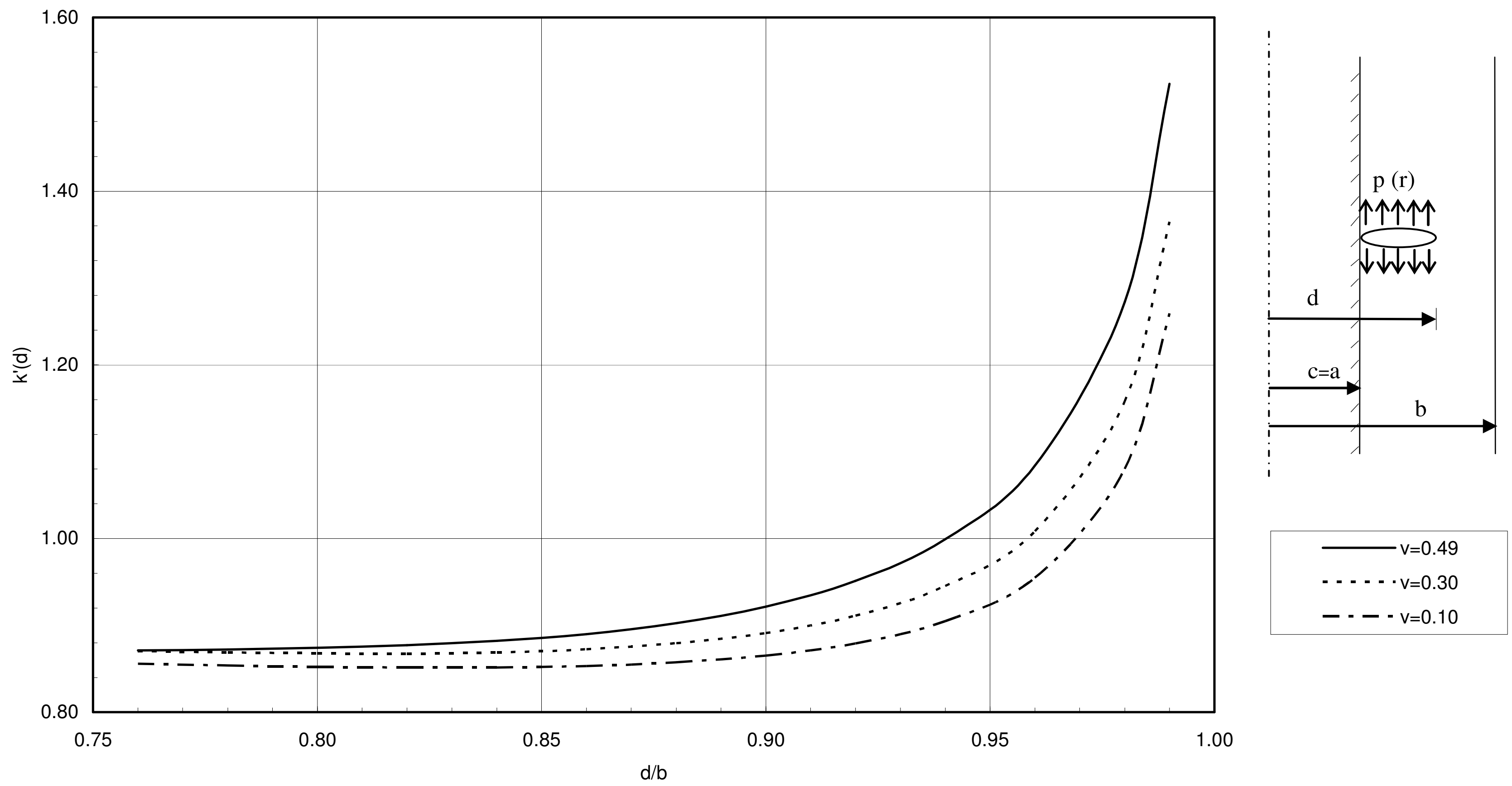

Figure 25. Variation of stress intensity factor k'(d) with c/b and ν for a crack terminating at the rigid cylinder (a/b=c/b=0.75).

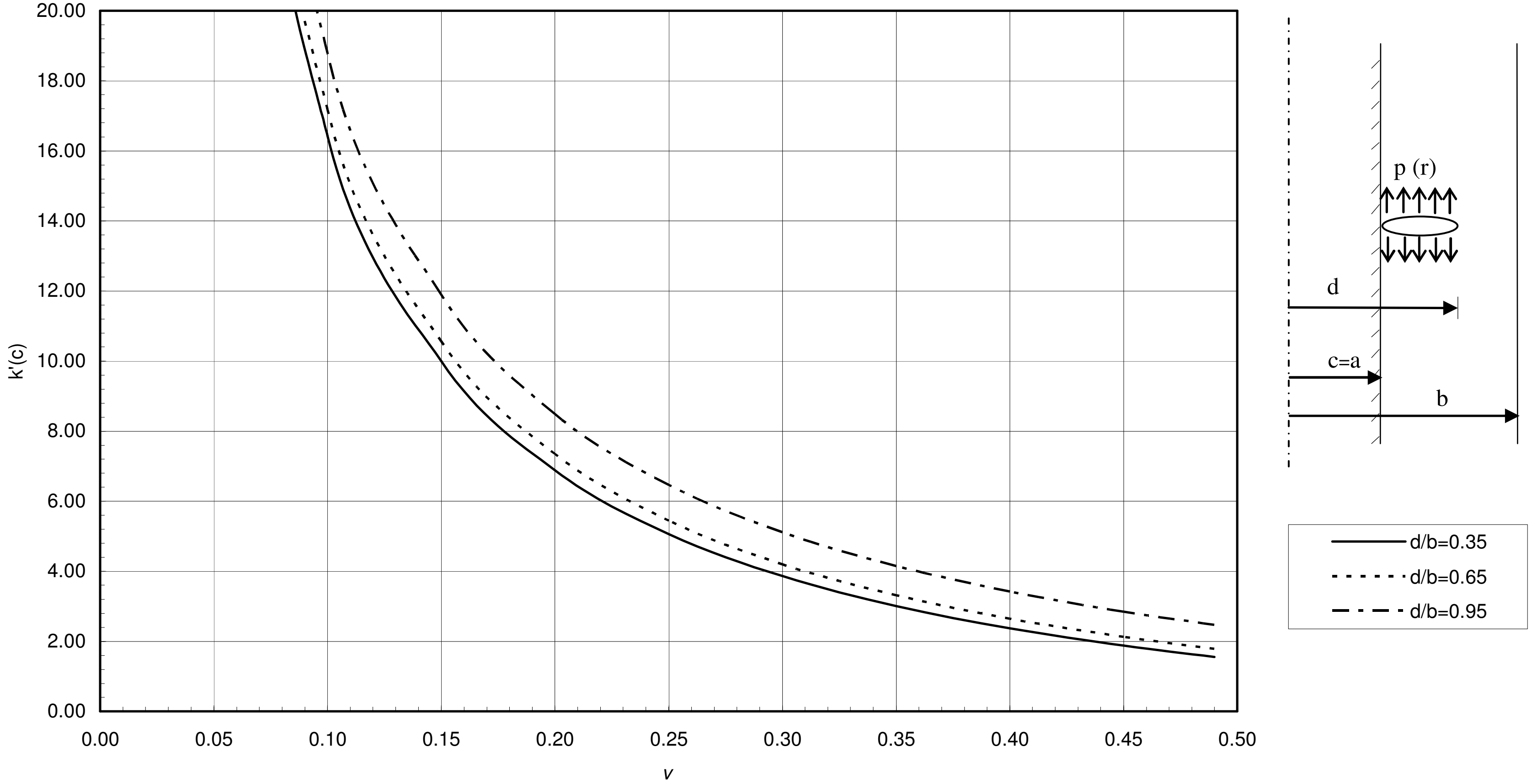

Figure 26. Variation of stress intensity factor k'(c) with ν for a crack terminating at the rigid cylinder (a/b=c/b=0.25).

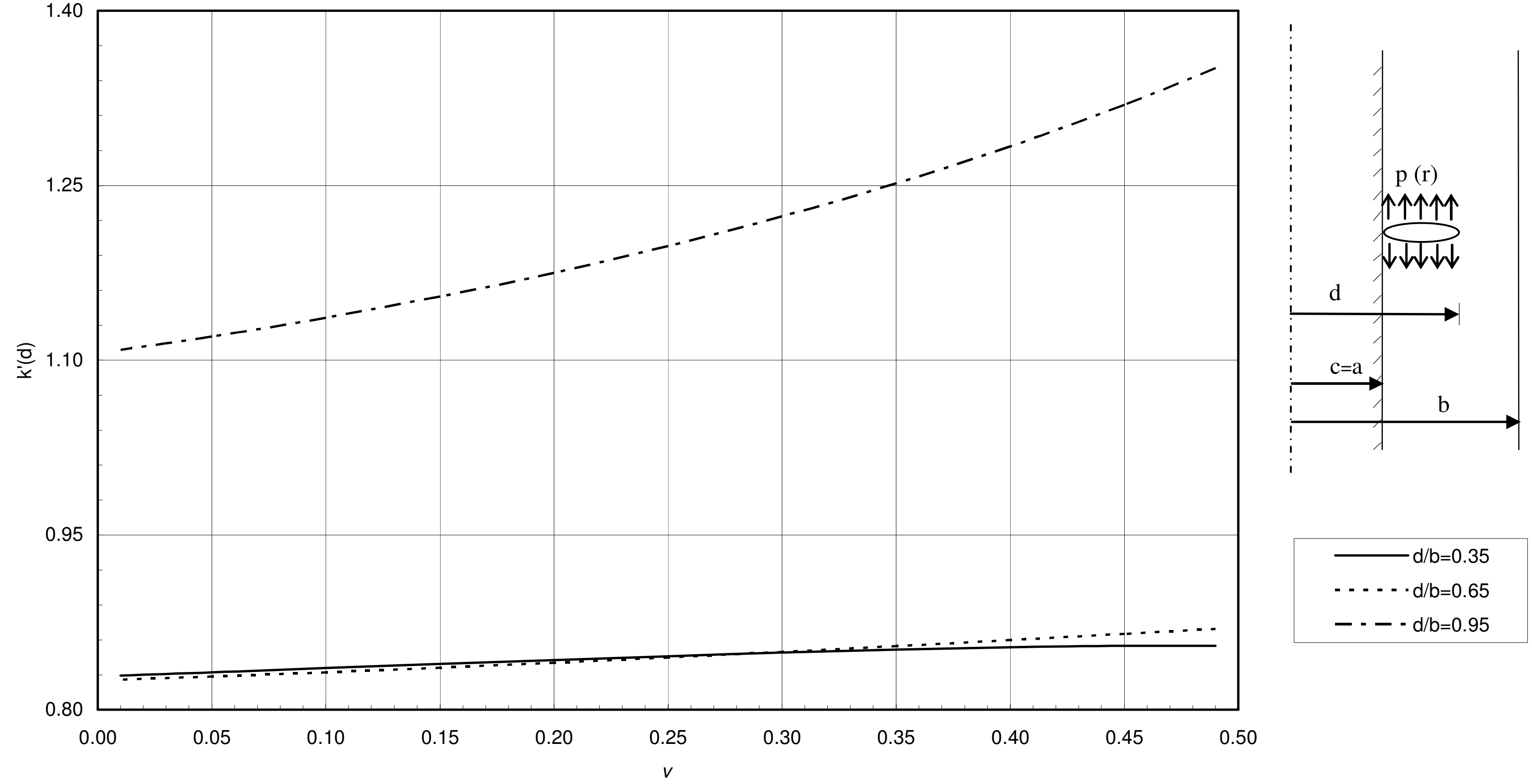

Figure 27. Variation of stress intensity factor k'(d) with ν for a crack terminating at the rigid cylinder (a/b=c/b=0.25).

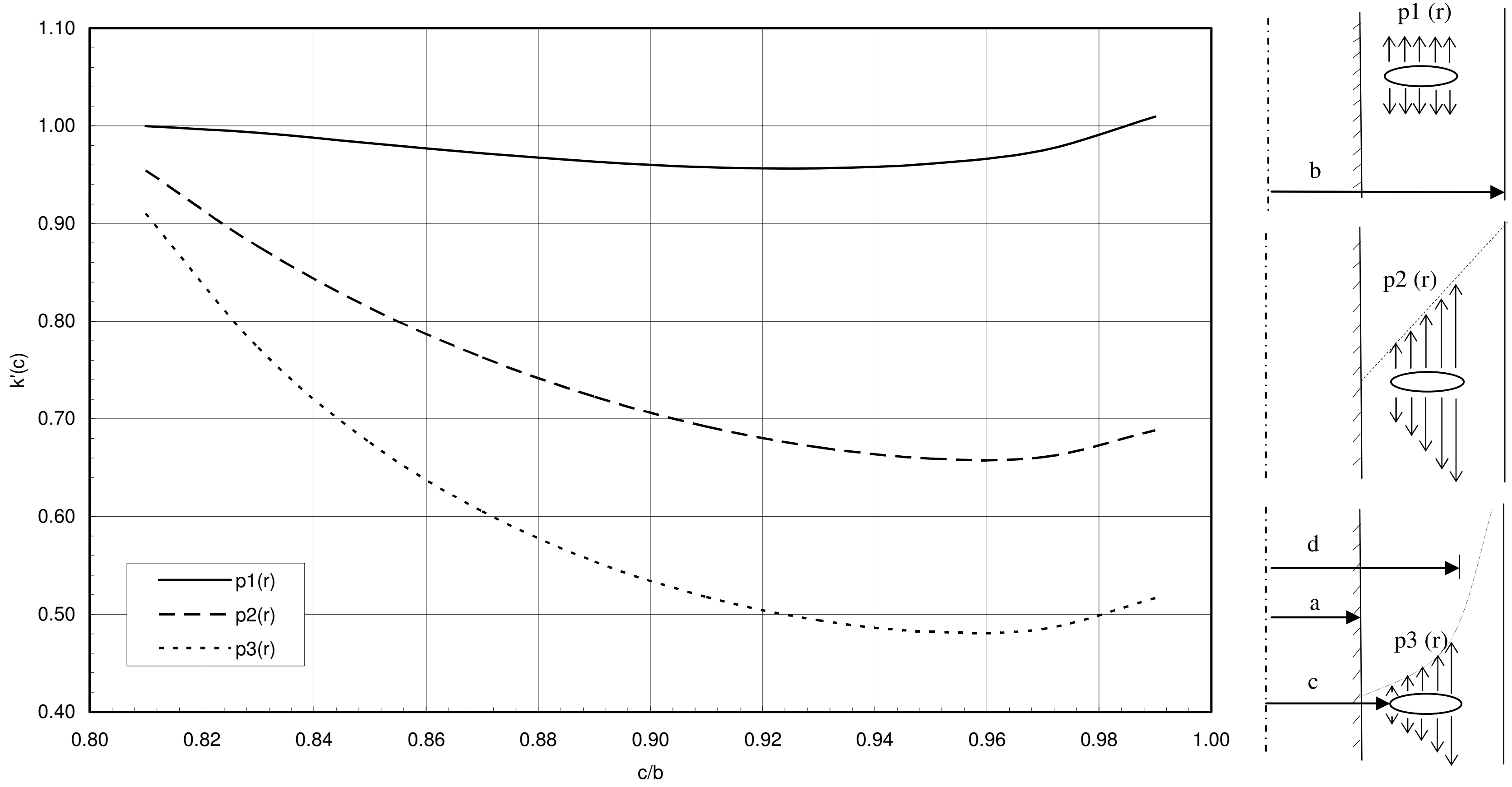

Figure 28. Variation of stress intensity factor k'(c) with c/b and different loads for an embedded crack (a/b=0.75, c/b=0.80).

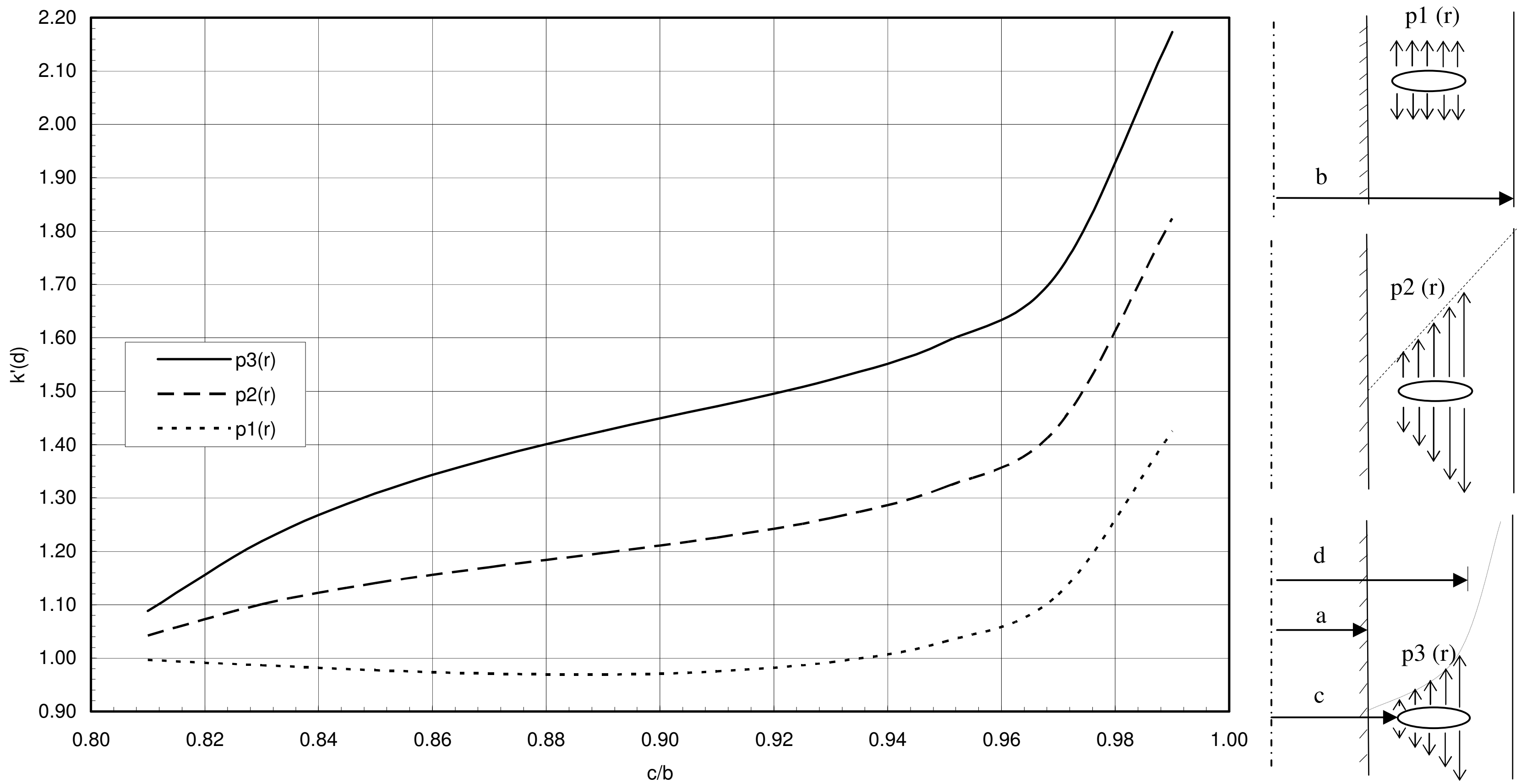

Figure 29. Variation of stress intensity factor k'(d) with c/b and different loads for an embedded crack (a/b=0.75, c/b=0.80).

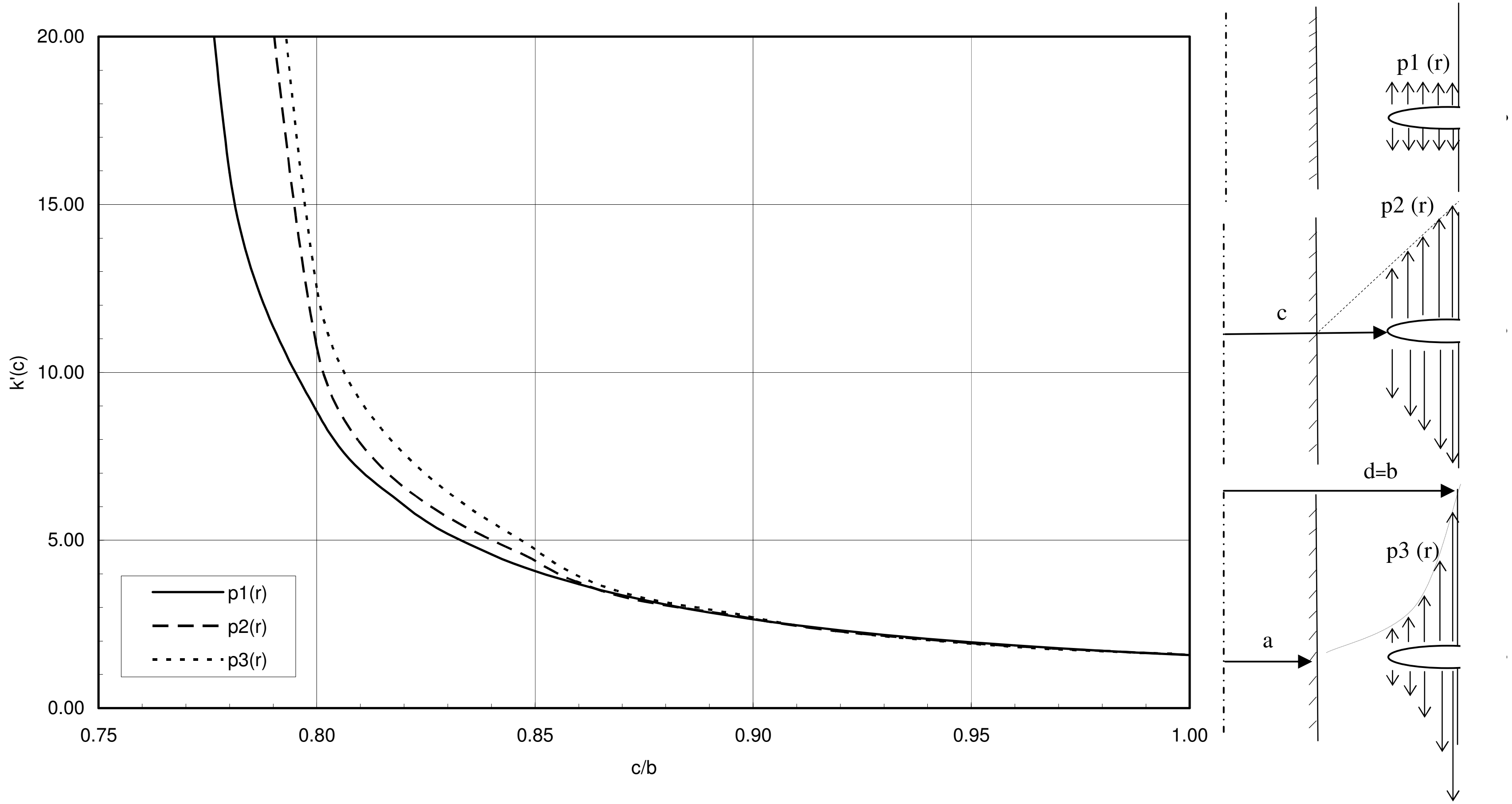

Figure 30. Variation of stress intensity factor k'(c) with c/b and different loads for an external edge crack (a/b=0.75, c/b=0.80).

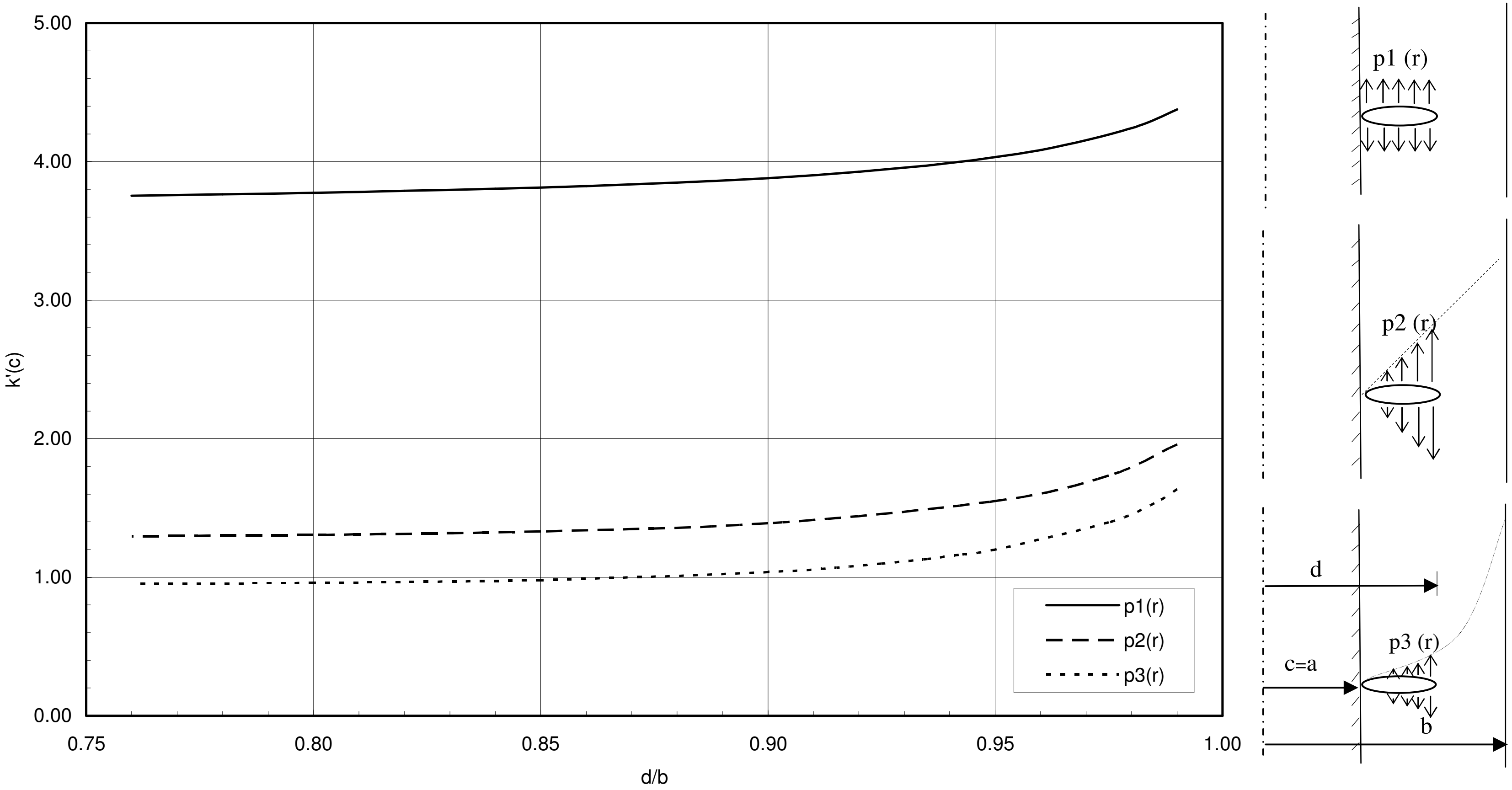

Figure 31. Variation of stress intensity factor k'(c) with c/b and different loads for a crack terminating at the rigid cylinder (a/b=0.75, c/b=0.80).

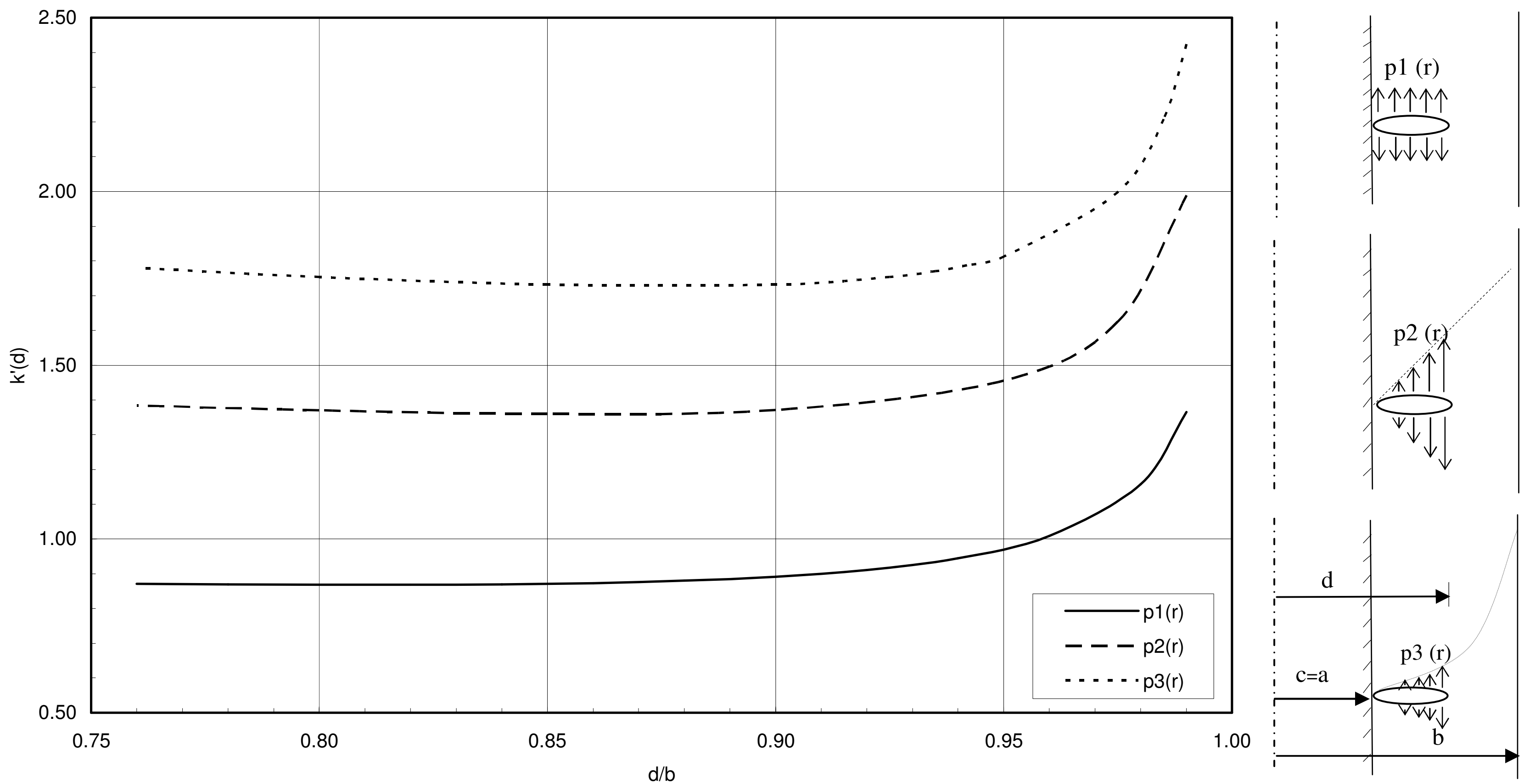

Figure 32. Variation of stress intensity factor k'(d) with c/b and different loads for a crack terminating at the rigid cylinder (a/b=0.75, c/b=0.80).

REFERENCES

1. Sneddon, I.N and Welch, J.T, “A note on the distribution of stress in a cylinder containing penny-shaped crack”, Int. J. Engineering Sci., Vol.1, pp.411-419, 1963.

2. W.D. Collins, “ Proc. Edinburgh Math.”, Soc. Vol.13,pp69-78,1962

3. Gupta, G.D., “The analysis of the semi-infinite cylinder problem“, Int. J. Solids and Structures, Vol.10, pp.137-148, 1974.

4. Geçit, M.R., “A cracked elastic strip bonded to a rigid support”, International Journal of Fracture., vol.14, No. 6, pp. 575-584, 1978

5. F. Erdogan, G.D. Gupta and T.S: Cook, “Numerical solution of singular integral equations, Methods of analysis and solutions of crack problems”, G.C. Sih., ed., Noordhoff, Leyden, 1973

6. Agarwal, V.K., “Axisymmetric solution of the end problem for semi-infinite elastic circular cylinder and its application to joined dissimilar cylinders under uniform tension” “, Int. J. Engineering Sci, Vol.16, pp.985-998, 1978.

7. Erdogan F. and Delale, H.F, “The stress intensity factor in hollow cylinder containing a radial crack”, Int. J. Fracture, Vol.20, pp.251-265, 1982.

8. Erdogan F. and Nied, H.F., “The elasticity problem for a thick-walled cylinder containing a circumferential crack”, Int. J. Fracture, Vol.22, pp.277-301, 1983.

9. H. Seçil Altundağ Artem and M.R. Geçit, "An elastic hollow cylinder under axial tension containing a crack and two rigid inclusions of ring shape", Computers and Structures, Vol.80, pp.2277-2287, 2002.

10. M. Evren Toygar and M.R. Geçit, "Cracked infinite cylinder with two rigid inclusions under axisymmetric tension", International Journal of Solids and Structures, 2005, article in press.

11. A. Birinci, "Axisymmetric crack problem of a thick-walled cylinder with cladding", International Journal of Engineering Science, Vol.40, pp.1729-1750, 2002

12. Geçit, M.R. and Turgut, A., "Extension of a finite strip bonded to a rigid support", Computational Mechanics, Vol.3, pp.398-410, 1988.

13. Abramowitz, M. And Stegun, I.A., Handbook of mathematical functions. Dover, 1965.

14. McLachan, N.W., Bessel functions for engineers, Oxford University Press, 1955.

15. Muskhelishvili, N.I., Singular integral equations., P. Noordhoff, Gröningen, Hollanf, 1953.

16. Cook, T.S and Erdogan, F., "Stress in bonded materials with a crack perpendicular to the interface ", Int.J. Engng. Sci., Vol.10, pp.677-697, 1972.

17. Stroud, A.H. and Secrest, D., "Gaussian quadrature formulas", Prentice-Hall, New York, 1966.

18. Gupta, G.D., "The problem of finite strip compressed between two rough rigid stamps ", Journal of Applied Mechanics, Vol.45, pp.281-286, 1978.

19. Erdelyi, A., Magnus, W., ed., “Tables of integral transforms”, vol.1,New York, McGraw-Hill, 1953

20. Ryshik, I.M.. and Gradstein, I.S., “Tables of series, products and integrals”, Academic Press, 1965.

21. Erdelyi, A., ed., “Higher transcendental functions”, vol.2, New York, McGraw-Hill, 1953

APPENDIX A

Evaluation of some integrals [19]:

$$\int_0^\infty e^{-\alpha z}\sin(\lambda z)dz=\frac{\lambda}{\lambda^2+\alpha^2} \quad ,$$

$$\int_0^\infty z e^{-\alpha z}\sin(\lambda z)dz=\frac{2\alpha\lambda}{(\lambda^2+\alpha^2)^2} \quad ,$$

$$\int_0^\infty z^2 e^{-\alpha z}\sin(\lambda z)dz=\frac{2\lambda(3\alpha^2-\lambda^2)}{(\lambda^2+\alpha^2)^3} \quad ,$$

$$\int_0^\infty e^{-\alpha z}\cos(\lambda z)dz=\frac{\alpha}{\lambda^2+\alpha^2} \quad ,$$

$$\int_0^\infty z e^{-\alpha z}\cos(\lambda z)dz=\frac{\alpha^2-\lambda^2}{(\lambda^2+\alpha^2)^2} \quad ,$$

$$\int_0^\infty z^2 e^{-\alpha z}\cos(\lambda z)dz=\frac{2\alpha(\alpha^2-3\lambda^2)}{(\lambda^2+\alpha^2)^3} \quad . \tag{A.1}$$

Using the following formulas [20], Eqs. (2.26) can be obtained.

$$\int_0^\infty \frac{\alpha}{\alpha^2+\lambda^2} J_0(a\alpha)J_0(t\alpha)d\alpha = I_0(a\lambda)K_0(t\lambda) \quad , \qquad (c \le t)$$

$$\int_0^\infty \frac{\alpha^2}{\alpha^2+\lambda^2} J_1(a\alpha)J_0(t\alpha)d\alpha = -\lambda I_0(a\lambda)K_0(t\lambda) \quad ,$$

$$\int_0^\infty \frac{\alpha}{\alpha^2+\lambda^2} J_1(a\alpha)J_1(t\alpha)d\alpha = I_1(a\lambda)K_1(t\lambda) \quad ,$$

$$\int_0^\infty \frac{\alpha^2}{\alpha^2+\lambda^2} J_0(a\alpha)J_1(t\alpha)d\alpha = \lambda I_0(a\lambda)K_0(t\lambda) \quad ,$$

$$\int_0^\infty \frac{\alpha}{\left(\alpha^2+\lambda^2\right)^2} J_0(a\alpha)J_0(t\alpha)d\alpha = \frac{1}{2\lambda}\left[-aI_1(a\lambda)K_0(t\lambda)+tI_0(a\lambda)K_1(t\lambda)\right] \quad ,$$

$$\int_0^\infty \frac{\alpha^2}{\left(\alpha^2+\lambda^2\right)^2} J_1(a\alpha)J_0(t\alpha)d\alpha = \frac{1}{2\lambda}\left[-\lambda aI_0(a\lambda)K_0(t\lambda)-\lambda tI_1(a\lambda)K_1(t\lambda)\right] \quad ,$$

$$\int_0^\infty \frac{\alpha}{\left(\alpha^2+\lambda^2\right)^2} J_1(a\alpha)J_1(t\alpha)d\alpha = \frac{1}{2\lambda}\left[-aI_0(a\lambda)K_1(t\lambda)-\frac{2}{\lambda}I_1(a\lambda)K_1(t\lambda)+tI_1(a\lambda)K_0(t\lambda)\right] \quad ,$$

$$\int_0^\infty \frac{\alpha}{\left(\alpha^2+\lambda^2\right)^2} J_0(a\alpha)J_1(t\alpha)d\alpha = \frac{1}{2\lambda}\left[-\lambda aI_1(a\lambda)K_1(t\lambda)+\lambda tI_0(a\lambda)K_0(t\lambda)\right] \quad . \qquad \text{(A.2)}$$

$$\int_0^\infty \frac{\alpha}{\alpha^2+\lambda^2} J_0(b\alpha)J_0(t\alpha)d\alpha = K_0(b\lambda)I_0(t\lambda) \quad , \qquad (d \geq t)$$

$$\int_0^\infty \frac{\alpha^2}{\alpha^2+\lambda^2} J_1(b\alpha)J_0(t\alpha)d\alpha = -\lambda K_1(b\lambda)I_0(t\lambda) \quad ,$$

$$\int_0^\infty \frac{\alpha}{\alpha^2+\lambda^2} J_1(b\alpha)J_1(t\alpha)d\alpha = K_1(b\lambda)I_1(t\lambda) \quad ,$$

$$\int_0^\infty \frac{\alpha}{\alpha^2+\lambda^2} J_0(b\alpha)J_1(t\alpha)d\alpha = -\lambda K_0(b\lambda)I_0(t\lambda) \quad ,$$

$$\int_0^\infty \frac{\alpha}{\left(\alpha^2+\lambda^2\right)^2} J_0(b\alpha)J_0(t\alpha)d\alpha = \frac{1}{2\lambda}\left[bK_1(b\lambda)I_0(t\lambda) - tK_0(b\lambda)I_1(t\lambda)\right] \quad ,$$

$$\int_0^\infty \frac{\alpha^2}{\left(\alpha^2+\lambda^2\right)^2} J_1(b\alpha)J_0(t\alpha)d\alpha = \frac{1}{2\lambda}\left[\lambda bK_0(b\lambda)I_0(t\lambda) - \lambda tK_1(b\lambda)I_1(t\lambda)\right] \quad ,$$

$$\int_0^\infty \frac{\alpha}{\left(\alpha^2+\lambda^2\right)^2} J_1(b\alpha)J_1(t\alpha)d\alpha$$
$$= \frac{1}{2\lambda}\left[bK_0(b\lambda)I_1(t\lambda) + \frac{2}{\lambda}K_1(b\lambda)I_1(t\lambda) - tK_1(b\lambda)I_0(t\lambda)\right],$$

$$\int_0^\infty \frac{\alpha}{\left(\alpha^2+\lambda^2\right)^2} J_0(b\alpha)J_1(t\alpha)d\alpha = \frac{1}{2\lambda}\left[-\lambda bK_1(b\lambda)I_1(t\lambda) + \lambda tK_0(b\lambda)I_0(t\lambda)\right] \quad .$$

(A.3)

APPENDIX B

Using the integral formulas given by (A.2) and (A.3) in Appendix A, F_1- F_4 appearing in Eqs. (2.27) become

$$F_1 = \int_0^\infty \left[-\frac{2a\lambda}{\kappa+1} I_1(a\lambda)K_1(t\lambda) + \frac{2t\lambda}{\kappa+1} I_0(a\lambda)K_0(t\lambda) + \frac{1}{t\lambda} - I_0(a\lambda)K_1(t\lambda) \right] tf(t)dt,$$

$$F_2 = \frac{4}{\kappa+1}\int_0^\infty \lambda\left[-bK_0(b\lambda)I_1(t\lambda) + tK_1(b\lambda)I_0(t\lambda)\right] tf(t)dt,$$

$$F_3 = \frac{1}{\kappa+1}\int_0^\infty \left[2a\lambda I_0(a\lambda)K_1(t\lambda) - 2t\lambda I_1(a\lambda)K_0(t\lambda) - (\kappa+1)I_1(a\lambda)K_1(t\lambda)\right] tf(t)dt,$$

$$F_4 = \frac{1}{\kappa+1}\int_0^\infty \left[\begin{array}{l} 2b\lambda K_0(b\lambda)I_1(t\lambda) - 2t\lambda K_1(b\lambda)I_0(t\lambda) \\ +(\kappa+1+2b^2\lambda^2)K_1(b\lambda)I_1(t\lambda) - 2bt\lambda^2 K_0(b\lambda)I_0(t\lambda) \end{array}\right] tf(t)dt, \quad \text{(B.1)}$$

The expression for the coefficients c_{11}-c_{44} appearing in Eq. (2.27) are as follows:

$$c_{11} = -(\kappa+1)a\lambda K_0(a\lambda) - \left(\frac{\kappa^2-1}{2} - 2b^2\lambda^2\right)K_1(a\lambda) - 2ab^2\lambda^3 K_0(b\lambda)H_{00} - a\lambda K_1(b\lambda)H_{01}(\kappa+1+2b^2\lambda^2),$$

$$c_{12} = \frac{1}{2}b\lambda K_1(a\lambda)H_{00}(\kappa^2-1) + \frac{1}{2}ab\lambda^2(\kappa-1)(K_0(a\lambda)H_{00} - K_1(a\lambda)H_{10}) - a\lambda\kappa K_1(b\lambda) + b^2\lambda^2 K_1(a\lambda)H_{01} + ab^2\lambda^3(K_0(a\lambda)H_{01} - K_1(a\lambda)H_{11}) - ab\lambda^2 K_0(b\lambda),$$

$$c_{13} = -K_1(b\lambda)H_{01} - \frac{1}{2}K_0(a\lambda)(4\kappa - 4b^2\lambda^2 - 3 - \kappa^2) + a\lambda K_1(a\lambda)(\kappa+1) - 2\kappa K_1(b\lambda)H_{01} + 2b^2\lambda^2(K_0(b\lambda)H_{00} + K_1(b\lambda)H_{01}) - \kappa^2 K_1(b\lambda)H_{01} + 2ab^2\lambda^3(K_0(b\lambda)H_{10} + K_1(b\lambda)H_{11}), + a\lambda(\kappa+1)K_1(b\lambda)H_{11} - 2b^2\lambda^2\kappa(K_0(b\lambda)H_{00} + K_1(b\lambda)H_{01})$$

$$c_{14} = -(\kappa+1)^2 K_1(a\lambda)H_{01} - 2b\lambda K_1(a\lambda)H_{00}(\kappa+1) - 2ab\lambda^2(K_0(a\lambda)H_{00} - K_1(a\lambda)H_{10}) - 2a\lambda K_1(b\lambda) + a\lambda(\kappa+1)(K_1(a\lambda)H_{11} - K_0(a\lambda)H_{01}),$$

$$c_{21} = -\frac{1}{2}(1+4b^2\lambda^2-\kappa^2)^2 I_1(a\lambda) + a\lambda I_1(b\lambda)H_{01}(\kappa+1) - 2ab^2\lambda^3(I_0(b\lambda)H_{00} - I_1(b\lambda)H_{01}) - a\lambda(\kappa+1)I_0(a\lambda)$$

$$c_{22} = -\frac{1}{2}b\lambda(1-\kappa^2)I_1(a\lambda)H_{00} - ab\lambda^2 I_0(b\lambda) + \frac{1}{2}ab\lambda^2(\kappa-1)(I_0(a\lambda)H_{00} + I_1(a\lambda)H_{10}) + a\lambda I_1(b\lambda) - b^2\lambda^2(\kappa+1)I_1(a\lambda)H_{01} + ab^2\lambda^3(I_0(a\lambda)H_{01} + I_1(a\lambda)H_{11})$$

$$c_{23} = (\kappa+1)^2 I_1(b\lambda)H_{01} - \frac{1}{2}(4\kappa+4b^2\lambda^2+3+\kappa^2)I_0(a\lambda) - a\lambda(\kappa+1)I_1(a\lambda) + 2b^2\lambda^2(\kappa+1)(I_1(b\lambda)H_{01} - I_0(b\lambda)H_{00}) - a\lambda(\kappa+1)I_1(b\lambda)H_{11} + 2ab^2\lambda^3(I_0(b\lambda)H_{10} - I_1(b\lambda)H_{11})$$

$$c_{24} = 2b\lambda(\kappa+1)I_1(a\lambda)H_{00} - 2ab\lambda^2(I_0(a\lambda)H_{00} + I_1(a\lambda)H_{10}) + 2a\lambda I_1(b\lambda) + (\kappa+1)^2 I_1(a\lambda)H_{01} - a\lambda(\kappa+1)(I_0(a\lambda)H_{01} + I_1(a\lambda)H_{11})$$

$$c_{31} = -(1+2b^2\lambda^2+\kappa)K_1(b\lambda)H_{11} + 2a\lambda K_0(a\lambda) + (\kappa+1)K_1(a\lambda) - 2b^2\lambda^2 K_0(b\lambda)H_{10}$$

$$c_{32} = -b\lambda(K_0(a\lambda)H_{11} + \frac{1}{2a\lambda}K_0(b\lambda)) - \frac{1}{2}b\lambda\kappa(K_0(a\lambda)H_{10} + K_1(a\lambda)H_{00})$$
$$+ab\lambda^2(K_1(a\lambda)H_{10} - K_0(a\lambda)H_{00}) + (\kappa+1)K_0(a\lambda)H_{11} - \frac{b^2\lambda}{a}K_1(b\lambda)$$
$$+a\lambda(K_0(a\lambda)H_{01} - K_1(a\lambda)H_{11})$$

$$c_{33} = (1+\kappa+2b^2\lambda^2)K_1(b\lambda)H_{01} + (\kappa+1)K_0(a\lambda) - 2a\lambda K_1(a\lambda) + 2b^2\lambda^2 K_0(b\lambda)H_{00}$$

$$c_{34} = -\frac{2b}{a}K_0(b\lambda) + (\kappa+1)(K_0(a\lambda)H_{11} + K_1(a\lambda)H_{01}) + 2a\lambda(K_0(a\lambda)H_{01} - K_1(a\lambda)H_{11})$$

$$c_{41} = -(1+2b^2\lambda^2+\kappa)I_1(b\lambda)H_{11} - 2a\lambda I_0(a\lambda) + (\kappa+1)I_1(a\lambda) + 2b^2\lambda^2 I_0(b\lambda)H_{10}$$

$$c_{42} = \frac{1}{2}b\lambda\kappa(I_0(a\lambda)H_{10} - I_1(a\lambda)H_{00}) + b\lambda(\frac{1}{2a\lambda}I_0(b\lambda) - I_0(a\lambda)H_{10}) - \frac{b^2\lambda}{a}I_1(b\lambda)$$
$$+ab\lambda^2(I_0(a\lambda)H_{00} + I_1(a\lambda)H_{10}) - (\kappa+1)I_0(a\lambda)H_{11} - a\lambda(I_0(a\lambda)H_{01} + I_1(a\lambda)H_{11})$$

$$c_{43} = -(\kappa+1)I_0(a\lambda) - 2a\lambda I_1(a\lambda) + (1+2b^2\lambda^2+\kappa)I_1(b\lambda)H_{01} - 2b^2\lambda^2 I_0(b\lambda)H_{00}$$

$$c_{44} = \frac{2b}{a}I_0(b\lambda) + (\kappa+1)(I_1(a\lambda)H_{01} - I_0(b\lambda)H_{11}) - 2a\lambda(I_0(a\lambda)H_{01} - I_1(b\lambda)H_{11})$$

$$D = (\kappa+1)^2 H_{01}H_{11} - \frac{2\kappa}{a\lambda} - 2a\lambda - \frac{2b^2\lambda}{a} - \frac{3}{2a\lambda} - \frac{\kappa^2}{2a\lambda} + 2b^2\lambda^2(\kappa+1)(H_{01}H_{11} - H_{00}H_{10})$$
$$+2ab^2\lambda^3(-H_{00}^2 + H_{10}^2 + H_{01}^2 - H_{11}^2) + a\lambda(\kappa+1)(H_{01}^2 - H_{11}^2) \tag{B.3}$$

where

$$H_{ij}(a\lambda, b\lambda) = K_i(a\lambda)I_j(b\lambda) + (-1)^{i+j+1}I_i(a\lambda)K_j(b\lambda) \qquad (i, j = 0, 1)$$

APPENDIX C

Integrals of Bessel functions are given in terms of the complete elliptic integrals K,E [19, 13, 21]

$$\int_0^\infty e^{-p\alpha} J_0(t\alpha) J_0(r\alpha) d\alpha = \frac{2}{\pi\sqrt{(t+r)^2+p^2}} K\left(\frac{2\sqrt{rt}}{\sqrt{(t+r)^2+p^2}}\right)$$

$$\int_0^\infty e^{-p\alpha} \alpha J_0(t\alpha) J_0(r\alpha) d\alpha = \frac{2p}{\pi\sqrt{(t+r)^2+p^2}\left[(t-r)^2+p^2\right]} E\left(\frac{2\sqrt{rt}}{\sqrt{(t+r)^2+p^2}}\right)$$

$$\int_0^\infty e^{-p\alpha} \alpha^2 J_0(t\alpha) J_0(r\alpha) d\alpha =$$

$$= \frac{2p^2}{\pi\left[(t+r)^2+p^2\right]^{3/2}\left[(t-r)^2+p^2\right]} \left\{ 2E\left(\frac{2\sqrt{rt}}{\sqrt{(t+r)^2+p^2}}\right) - K\left(\frac{2\sqrt{rt}}{\sqrt{(t+r)^2+p^2}}\right) \right\}$$

$$- \frac{2\left[(t-r)^2-p^2\right]}{\pi\sqrt{(t+r)^2+p^2}\left[(t-r)^2+p^2\right]} E\left(\frac{2\sqrt{rt}}{\sqrt{(t+r)^2+p^2}}\right)$$

$$\int_0^\infty e^{-p\alpha} J_1(r\alpha) J_1(r\alpha) d\alpha =$$

$$= \frac{t^2+r^2+p^2}{\pi tr\sqrt{(t+r)^2+p^2}} \left\{ K\left(\frac{2\sqrt{rt}}{\sqrt{(t+r)^2+p^2}}\right) - \left(\frac{(t+r)^2+p^2)}{\pi tr\sqrt{(t+r)^2+p^2}}\right) E\left(\frac{2\sqrt[2]{tr}}{\sqrt{(t+r)^2+p^2}}\right) \right\}$$

$$\int_0^\infty e^{-p\alpha}\alpha J_1(r\alpha)J_1(r\alpha)d\alpha == \frac{p(t^2+r^2+p^2)}{\pi r\sqrt{(t+r)^2+p^2}\left[(t-r)^2+p^2\right]}E\left(\frac{2\sqrt{rt}}{\sqrt{(t+r)^2+p^2}}\right)$$

$$-\frac{p}{\pi r\sqrt{(t+r)^2+p^2}}K\left(\frac{2\sqrt{rt}}{\sqrt{(t+r)^2+p^2}}\right)$$

$$\int_0^\infty e^{-p\alpha}\alpha^2 J_1(t\alpha)J_1(r\alpha)d\alpha=$$

$$=\frac{p^2(t^2+r^2)+(t^2-r^2)^2}{\pi r\left[(t+r)^2+p^2\right]^{3/2}\left[\left((t-r)^2+p^2\right)\right]}+K\left(\frac{2\sqrt{rt}}{\sqrt{(t+r)^2+p^2}}\right)$$

$$+\frac{1}{\pi r\sqrt{(t+r)^2+p^2}}\left[\frac{4p^2+(p^2+r^2+t^2)^2}{\left[(t+r)^2+p^2\right]\left[(t+r)^2+p^2\right]}\right]E\left(\frac{2\sqrt{rt}}{\sqrt{(t+r)^2+p^2}}\right)$$

$$-\frac{1}{\pi r\sqrt{(t+r)^2+p^2}}\left[\frac{(t^2+r^2+4p^2)}{(t-r)^2+p^2}\right]E\left(\frac{2\sqrt{rt}}{\sqrt{(t+r)^2+p^2}}\right)$$

$$\int_0^\infty e^{-p\alpha}J_0(t\alpha)J_1(r\alpha)d\alpha=\frac{1}{\pi r\sqrt{(t+r)^2+p^2}}K\left(\frac{2\sqrt{tr}}{\sqrt{(t+r)^2+p^2}}\right)$$

$$+\left(\frac{(r^2-t^2-p^2}{\pi r\sqrt{(t+r)^2+p^2}\left[(t-r)^2+p^2\right]}\right)E\left(\frac{2\sqrt{tr}}{\sqrt{(t+r)^2+p^2}}\right),$$

$$\int_0^\infty e^{-p\alpha}\alpha^2 J_0(t\alpha)J_1(r\alpha)d\alpha=$$

$$=\frac{p(r^2-t^2-p^2)+(t^2-r^2)^2}{\pi r\left[(t+r)^2+p^2\right]^{3/2}\left[\left((t-r)^2+p^2\right)\right]}+\left\{2E\left(\frac{2\sqrt{rt}}{\sqrt{(t+r)^2+p^2}}\right)-K\left(\frac{2\sqrt{rt}}{\sqrt{(t+r)^2+p^2}}\right)\right\}$$

$$+\frac{p\left[(r^2-t^2-p^2\right]}{\pi r\sqrt{(t+r)^2+p^2}\left((t-r)^2+p^2\right)^2}E\left(\frac{2\sqrt{rt}}{\sqrt{(t+r)^2+p^2}}\right)$$